

Caspase Cleavage of Keratin 18 and Reorganization of Intermediate Filaments during Epithelial Cell Apoptosis

Carlos Caulín, Guy S. Salvesen, and Robert G. Oshima

The Burnham Institute (formerly the La Jolla Cancer Research Foundation), La Jolla, California 92037

Abstract. Keratins 8 (K8) and 18 (K18) are major components of intermediate filaments (IFs) of simple epithelial cells and tumors derived from such cells. Structural cell changes during apoptosis are mediated by proteases of the caspase family. During apoptosis, K18 IFs reorganize into granular structures enriched for K18 phosphorylated on serine 53. K18, but not K8, generates a proteolytic fragment during drug- and UV light-induced apoptosis; this fragment comigrates with K18 cleaved in vitro by caspase-6, -3, and -7. K18 is cleaved by caspase-6 into NH₂-terminal, 26-kD and COOH-terminal, 22-kD fragments; caspase-3 and -7 additionally cleave the 22-kD fragment into a 19-kD fragment. The cleavage site common for the three caspases was the sequence VEVD/A, located in the

conserved L1-2 linker region of K18. The additional site for caspases-3 and -7 that is not cleaved efficiently by caspase-6 is located in the COOH-terminal tail domain of K18. Expression of K18 with alanine instead of serine at position 53 demonstrated that cleavage during apoptosis does not require phosphorylation of serine 53. However, K18 with a glutamate instead of aspartate at position 238 was resistant to proteolysis during apoptosis. Furthermore, this cleavage site mutant appears to cause keratin filament reorganization in stably transfected clones. The identification of the L1-2 caspase cleavage site, and the conservation of the same or very similar sites in multiple other intermediate filament proteins, suggests that the processing of IFs during apoptosis may be initiated by a similar caspase cleavage.

APOPTOSIS, or programmed cell death, is a process that enables multicellular organisms to eliminate cells that are damaged or mislocated or have become superfluous (Ellis et al., 1991). Failure of cells to undergo appropriate apoptotic cell death is involved in a variety of human diseases including autoimmune disease, viral infections, and cancer (Thompson, 1995). Apoptosis also provides an orderly way to render the contents of superfluous cells benign and packaged for further degradation. The apoptosis of epithelial cells presents a significant problem of disposal of intermediate filament cytoskeletal components, which are highly polymerized and are relatively insoluble in normal aqueous solutions. Packaging of the extended, intermediate filament cytoskeleton into apoptotic bodies is a process that is likely necessary for nearly all mammalian cells.

Apoptosis is characterized by ultrastructural changes that include actin cytoskeletal disruption, membrane blebbing, decreases in adhesion and intercellular contacts, chromatin condensation, nuclear fragmentation, and packaging of the nuclear fragments into membrane-enclosed apoptotic bodies (Wyllie et al., 1980). Biochemical changes

include limited proteolysis of cellular proteins by the caspase family of cysteine proteases (Alnemri et al., 1996) that are mediators of apoptotic cell death (Martin and Green, 1995; Kumar and Lavin, 1996). Genetic evidence that supports the involvement of caspases in apoptosis includes the requirement of CED-3, a protease homologous to the mammalian interleukin-converting enzyme (ICE) (Yuan et al., 1993), for cell death during development of *Caenorhabditis elegans*. In mammals, ectopic expression of members of the caspase family results in apoptosis (Miura et al., 1993), while expression of CrmA and p35, viral inhibitors of caspases (Ray et al., 1992; Bump et al., 1995), can suppress apoptosis (Rabizadeh et al., 1993; Gagliardini et al., 1994). At least 10 members of the caspase family have been identified to date. One distinctive feature of these proteases is the requirement of an aspartate adjacent to the cleavage site (position P1, where P4P3P2P1/P1' indicates the position of residues relative to the cleavage site) (Howard et al., 1991). The cellular targets for caspases now include over a dozen individual proteins as diverse as transcription factors and actin (Casciola-Rosen et al., 1994; Lazebnik et al., 1994; Brancolini et al., 1995; Emoto et al., 1995; Cryns et al., 1996; Janicke et al., 1996; Kayalar et al., 1996; Na et al., 1996; Song et al., 1996; Takahashi et al., 1996; Wang et al., 1996; Gu et al., 1997). Lamins are one of the better-characterized targets for

Address all correspondence to Robert G. Oshima, The Burnham Institute, 10901 N. Torrey Pines Road, La Jolla, CA 92037. Tel.: (619) 646-3147. Fax: (619) 646-3193. e-mail: rgoshima@jcrf.edu

caspases. They constitute the main structural components of the lamina underlying the nuclear membrane. Apoptosis induced by several stimuli results in the proteolytic cleavage of lamins to facilitate the nuclear collapse that is characteristic of apoptosis (Rao et al., 1996). Caspase-6 (Mch-2) appears selective for cleaving lamins A and C in the linker region of the α helical domain after the aspartic acid in the sequence VEID/N (Takahashi et al., 1996). Lamin B is cleaved in the sequence VEVD/S (Rao et al., 1996).

Intermediate filaments (IFs)¹ are composed of members of a family of proteins that organize to form 10-nm filaments and share sequence homology and structural features (Fuchs and Weber, 1994). IF proteins have a large central α helical rod domain broken by three short linker regions and are flanked by variable nonhelical NH₂ and COOH-terminal domains. IF proteins are classified into five groups: type I, acidic keratins (K9-K20); type II, basic keratins (K1-K8); type III, vimentin, desmin, GFAP, and peripherin; type IV, neurofilaments, nestin, and internexin; and type V, lamins. Higher eukaryotes express IF proteins in a tissue- and differentiation-specific manner (Steinert and Roop, 1988). Keratins are obligate heteropolymers that constitute the IFs of epithelial cells by the association of at least one type I and one type II keratin (Steinert et al., 1976; Hatzfeld and Franke, 1985). Keratin 8 (K8) and keratin 18 (K18) are the major components of IFs of simple or single layer epithelial tissues. The expression of these proteins is generally persistent in carcinomas arising from tissues that normally express K8 and K18 (Schaafsma et al., 1990; Trask et al., 1990; Schussler et al., 1992; Oshima et al., 1996). The mouse form of K8 is essential for normal development; its absence results in midgestational embryonic lethality in one genetic background and partial embryonic lethality, female sterility, and adult colorectal hyperplasia in a different genetic background (Baribault et al., 1993, 1994). Transgenic expression of a dominant acting mutant form of K18 results in liver dysfunction (Ku et al., 1995) and increased sensitivity to both griseofulvin and acetaminophen (Ku et al., 1996b). K8 and K18 have also been implicated in drug resistance (Bauman et al., 1994; Parekh and Simpkins, 1995; Anderson et al., 1996) and alterations in invasive behavior (Chu et al., 1993, 1996; Pankov et al., 1997). Both K8 and K18 are subject to posttranslational modifications by phosphorylation (Oshima, 1982; Ku and Omary, 1994; Ku et al., 1996a). K18 can be phosphorylated on serines by several kinases in vitro. In vivo, the major phosphorylation site is on serine 53 (previously referred to as serine 52 relative to posttranslational processed protein) (Ku and Omary, 1994). Phosphorylation of K18 on serine 53 has been implicated in increased solubility and altered polymerization (Ku and Omary, 1994), differential localization within hepatocytes (Liao et al., 1995a), association with proteins of the 14-3-3 family (Liao and Omary, 1996), and with cellular stress (Ku et al., 1996a). Increased phosphorylation of K18 has also been linked recently to the reorganization of hepatocyte keratin filaments subjected to the toxin microcystin LR (Toivola et al., 1997).

¹. Abbreviations used in this paper: DAPI, 4, 6-diamidino-2-phenylindole; IF, intermediate filament; K8 and K18, keratins 8 and 18.

In this study, we show that K8/K18 filaments are dramatically reorganized during apoptosis, and that this reorganization is associated with the phosphorylation of K18 on serine 53. Furthermore, K18, but not K8, is cleaved by caspases at the sequence VEVD/A within the region that links two major α helical domains shared by all IF proteins. This cleavage may initiate the orderly processing of the filament proteins during apoptosis in epithelial cells.

Materials and Methods

Cell Lines, Plasmids, and Antibodies

SNG-M cells are from a human endometrial adenocarcinoma (Ishiwata et al., 1977). HR-9 cells are mouse parietal endodermal cells (Chung et al., 1977). Cells were maintained in DME supplemented with 10% FCS and gentamycin sulfate (30 μ g/ml).

Plasmid pK187 consists of the full-length K18 cDNA cloned into the EcoRI site of pGEM1 with the 5' end proximal to the T7 RNA polymerase promoter (Oshima et al., 1986). pK811 consists of the full-length K8 cDNA cloned into the EcoRI site of pGEM1 with the 5' end proximal to the T7 RNA polymerase promoter (Kulesh et al., 1989). SP64B7 consists of the full-length EndoB (mouse K18) cDNA (Trevor and Oshima, 1985; Singer et al., 1986) cloned into the SP64 plasmid. Plasmid pGC1853 contains the human K18 gene cloned into the HindIII site of pGEM1 (Kulesh and Oshima, 1988). pGC1853-K18S15A contains the mutation ser53 \rightarrow ala (Liao et al., 1995a) within the context of the K18 gene. This was a very generous gift from Dr. Bishr Omary (Stanford University School of Medicine, Stanford, CA). pCIN-K18-D238E contains the K18 cDNA with the mutation asp238 \rightarrow glu cloned into the EcoRI site of the pCIN4 expression vector (Rees et al., 1996).

We used the following antibodies: rabbit polyclonal antibody 1589 against EndoB, which cross-reacts with K18 and was prepared, characterized, and reacts like the originally described antiserum (Oshima, 1981). The rat monoclonal antibody TROMA1 binds EndoA but not EndoB (Brulet et al., 1980; Oshima, 1982). The monoclonal antibodies, CK5 specific for K18 and M20 against K8, were purchased from Sigma Chemical Co. (St. Louis, MO). The 3055 rabbit polyclonal antibody specific for K18 phosphorylated on serine 53 has been previously described (Liao et al., 1995a).

Full-length cDNAs encoding caspases-3, -6, and -7 were cloned into pET vectors (Invitrogen, San Diego, CA) and expressed in *Escherichia coli* strain BL21 (DE3)pLysS (Orth et al., 1996). The constructs contained COOH-terminal His6-tags to allow for purification by affinity chromatography on Ni²⁺-NTA-agarose (Qiagen, Chatsworth, CA) or Pharmacia LKB Biotech., Inc. (Piscataway, NJ) chelating Sepharose charged with NiSO₄ according to the manufacturer's instructions. The caspases were obtained predominantly as the active two chain forms, with yields of 0.5–1.0 mg/liter of induced culture, and were judged to be >95% pure by SDS-PAGE and NH₂-terminal sequence analysis. Caspase concentrations were determined from their observed absorbance at 280 nm and from the calculated molar extinction coefficient (Edelhoch, 1967).

Immunofluorescence

SNG-M cells grown on coverslips were treated with etoposide (250 μ g/ml) or DMSO solvent alone for 24 h, washed three times in PBS, and fixed in methanol for 5 min (-20° C). Coverslips were washed three times in PBS, treated with PBS containing 0.1% Triton X-100 for 4 min, washed three times with PBS, blocked with 1 mg/ml ovalbumin for 30 min, and incubated for 1 h with primary antibody (CK5 or 3055). Cells were washed twice in PBS containing 0.1% Tween 20, twice in PBS, incubated in PBS containing 1 mg/ml ovalbumin for 15 min, and with FITC-labeled secondary antibody for 30 min. The cells were then washed twice in PBS containing 0.1% Tween 20 and twice in PBS. To visualize DNA, coverslips were incubated in 30 μ g/ml propidium iodide for 5 min and washed once in PBS. Coverslips were mounted over slides with Vectashield mounting medium (Vector Laboratories, Burlingame, CA) and were visualized in either a confocal microscope (model LSM 410; Carl Zeiss, Inc., Thornwood, NY) or a fluorescence microscope (model Axiovert 405; Carl Zeiss, Inc.). With the confocal microscope, 12 optical sections were integrated for each photo. Images were captured on film with the Axiovert micro-

scope, and the negatives were scanned. Figures were printed with the use of Adobe Photoshop software (San Jose, CA).

In Vitro Transcription and Translation of K8, K18, and EndoB

K8 and K18 proteins were synthesized using separated or coupled transcription and translation reactions as indicated. Transcription was performed using 2 µg of linearized plasmid DNA (XbaI for pK811, HindIII for pK187, and BamHI for SP64B7) in a 50-µl volume as previously described (Oshima et al., 1986). 1 µg of RNA was used for translation using a rabbit reticulocyte lysate system (Promega Corp., Madison, WI), following the instructions of the supplier with 2 µl of translation grade [³⁵S]methionine (1,200 Ci/mmol at 10 mCi/ml) (New England Nuclear, Wilmington, DE) in a 25-µl reaction for 1 h at 30°C. Coupled transcription/translation was performed using the TNT kit (Promega Corp.) using 2 µg of linearized plasmid DNA in the presence of 50 µCi of radioactive methionine in a 50-µl reaction for 2 h at 30°C. Reaction products were stored at -20°C. Truncated versions of K18 were generated from the pK187 plasmid digested with BamHI for K18-339, and ScaI for K18-269. Truncated forms of EndoB were generated from the SP64B7 plasmid digested with AvaI for EndoB-316, ScaI for EndoB-262, and PvuII for EndoB-191.

K18 and EndoB In Vitro Cleavage Assay

1 µl of the radioactive translation product was incubated with 1 µl of purified recombinant caspase-6 (0.2 mg/ml), caspase-3 (0.15 mg/ml), or caspase-7 (0.13 mg/ml) at the indicated dilutions in a 40-µl volume containing 50 mM Hepes, 0.1 M NaCl, 10% sucrose, 0.1% CHAPS, and 10 mM DTT at 37°C for the indicated times. Reaction was stopped by adding SDS-PAGE sample buffer (Laemmli, 1970). Cleavage products were analyzed by SDS-PAGE and fluorography.

Site-directed Mutagenesis

Site-directed mutagenesis of the aspartate to glutamate at position 238 of K18 was achieved using the QuickChange™ Site-Directed Mutagenesis Kit (Stratagene, La Jolla, CA) following the instructions of the supplier. The two complementary oligonucleotides, GTTGACCGTGGAGGTA-GAGGCCCAAACTTCAGG and CCTGAGATTGGGGCCTCTACCTCCACGGTCAAC, containing the desired mutation were used. A 50-µl reaction was subjected to 12 cycles of 95°C 30 s, 55°C 1 min, and 68°C 10 min. 10 U of DpnI restriction enzyme was added to each amplification reaction and were incubated for 1 h at 37°C. The reaction was used to transform Epicurean Coli XL1-blue competent cells. Plasmid DNA was purified from seven colonies and sequenced. All seven plasmids contained the desired mutation without other changes.

Gel Electrophoresis and Immunoblotting

Cells were lysed in SDS-PAGE sample buffer, and equal amounts of protein were separated on 15% polyacrylamide gels. Proteins were transferred electrophoretically to nitrocellulose (Towbin et al., 1979) (12–15 h, 75 mA). Membranes were blocked by incubation in 5% nonfat dry milk with 0.1% Tween 20 in PBS for 2 h at room temperature. After washing four times in PBS containing 0.1% Tween 20 for 25 min, membranes were incubated with primary antibody diluted in blocking buffer (1:5,000 for 1589, 1:2,000 for M20, and 1:500 for 3055) for 1 h at room temperature. After washing, the membranes were incubated with secondary antibody diluted in blocking buffer (1:7,500 horseradish peroxidase-labeled anti-rabbit Ig for 1589 and 3055, and 1:10,000 horseradish peroxidase-labeled antimouse Ig for M20) for 1 h at room temperature, washed again four times in PBS containing 0.1% Tween 20 for 25 min, and detected using the enhanced chemiluminescence system (Amersham Corp., Arlington Heights, IL) following the directions of the supplier.

Apoptosis Assays

Apoptosis was induced by UV irradiation from a Stratalinker (Stratagene) UV source by exposing cells in complete medium to 120 millijoules of UV light. Apoptosis was also induced by treatment of semiconfluent cultures with the drugs etoposide (Sigma Chemical Co.) at 250 µg/ml for SNG-M and 125 µg/ml for HR-9 and daunomycin (Sigma Chemical Co.) at 6 µg/ml for SNG-M and 2 µg/ml for HR-9.

Apoptosis was confirmed using two approaches. First, DNA degrada-

tion was observed by agarose gel electrophoresis. Low molecular weight genomic DNA was extracted from adherent and floating cells induced to undergo apoptosis (Frisch and Francis, 1994). PBS-washed, floating, or adherent cells were suspended in 0.5% Triton X-100, 10 mM EDTA, 10 mM Tris, pH 7.4, and incubated for 12–16 h at 4°C. After centrifugation at 13,000 g for 30 min, the supernatants were incubated with 20 µg/ml RNase A for 30 min at 37°C, extracted with phenol-chloroform, and analyzed in 1.4% agarose gels in Tris-borate-EDTA buffer. In addition, the ratio of apoptotic and normal cells in cell cultures was determined by staining the cell nuclei with 4, 6-diamidino-2-phenylindole (DAPI). Floating cells were harvested by centrifugation at 1,500 g for 5 min, washed with PBS, and resuspended in PBS. Adherent cells were exposed to trypsin and EDTA, centrifuged at 1,500 g for 5 min, washed with PBS, resuspended in PBS, and mixed with floating cells. Cells were then fixed with methanol (-20°C) for 5 min. One drop of the cell suspension was placed on a cover-slip, air dried, and DAPI (2 µg/ml) was applied over the cells. Normal and fragmented nuclei were counted using a fluorescence microscope (Dialux 20; E. Leitz, Inc., Rockleigh, NJ).

Cell Transfections

HR-9 cells were transfected by the calcium phosphate precipitate method as described previously (Oshima et al., 1990). pGC1853 and pGC1853-K18S15A were cotransfected with pPGK-Neo as a selectable plasmid at a 10:1 molar ratio. Stable transfected clones were selected by incubation with 400 µg/ml G418. Cells with K18 expression were identified by indirect immunofluorescent staining with monoclonal antibody CK5, specific for human K18.

Results

Reorganization of K8/K18 Filaments During Apoptosis

K8 and K18 are the characteristic IF proteins expressed in simple epithelia. The two proteins form heterodimers that polymerize to generate IFs and bundles of IFs that normally extend from the nucleus to the plasma membrane. When the epithelial cell line SNG-M is treated with etoposide for 24 h, apoptotic cells begin to detach from the dish. Most of the cells that remained attached after this length of drug treatment contained a normal cytoskeletal network pattern (Fig. 1, A, C, and E). The nuclear morphology of these cells was normal (Fig. 1, B, D, and F). However, a small percentage of the cells had alterations in the organization of the K18 filament network. Some cells showed a K18 cytoskeleton in which the filament network appeared aggregated or collapsed, and others contained K18 in aggregates or spots spread throughout the cytoplasm (Fig. 1, A, C, and E). A gradation in the size of the granules was observed between different cells. Cells could be detected with K18 organized in both small spots still associated with the filament network (Fig. 1 A) and as large granules (Fig. 1 E). Most of the cells with disorganized keratin patterns contained fragmented nuclei, a characteristic of advanced apoptosis (Fig. 1 E, lower right corner). All of the cells with fragmented nuclei contained granular K18 organization. However, not every cell with disorganized filaments had fragmented nuclei, which suggests that the reorganization of K18 filaments is an event that occurs before obvious nuclear fragmentation. Furthermore, some cells had both a few granules and extended filament bundles, suggesting that keratin granule formation may start locally within a portion of the cell.

Cells were also stained with fluorescent annexin V, a marker that reflects the membrane changes that occur early during apoptosis (Thiagarajan and Tait, 1990; Martin et al., 1995). In SNG-M cells treated with etoposide for 24 h,

K18

DNA

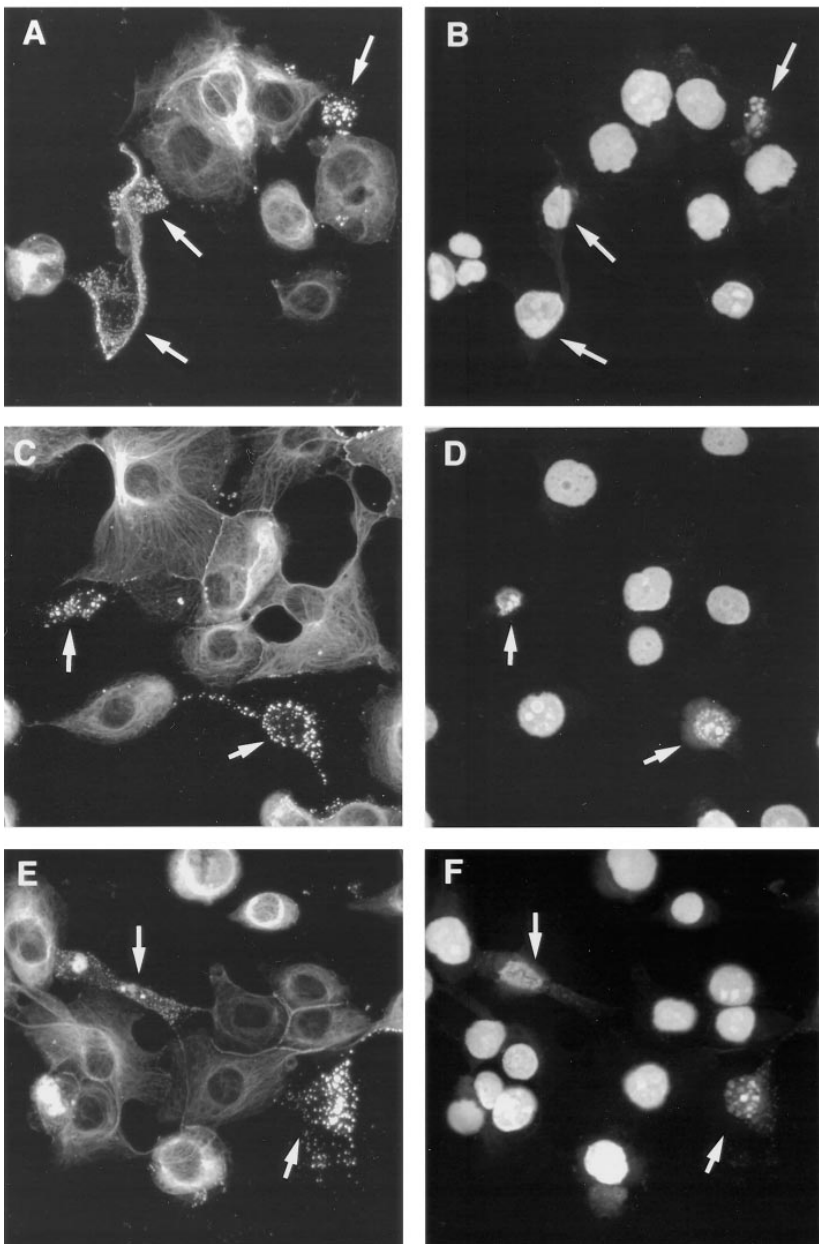


Figure 1. Induction of apoptosis in SNG-M cells results in reorganization of K18 IF. SNG-M cells were treated with etoposide (250 µg/ml) for 24 h and stained by indirect immunofluorescence for K18 with monoclonal antibody CK5 (A, C, and E) and with propidium iodide for DNA (B, D, and F). Images were analyzed with a confocal microscope. Note the granular K18 staining associated with altered nuclear morphology.

the number of cells stained with annexin V was greater than the number of cells with K18 granules (data not shown). Many of the cells stained with annexin V had a perfectly organized K18 filament network. These observations suggest alterations in the membrane, as reflected by annexin V binding, precede K18 filament collapse and nuclei fragmentation in this order. Intermediate filament disorganization and reorganization during mitosis is associated with phosphorylation. It has been shown that one primary phosphorylation site on K18 is serine 53 (Ku and Omari, 1994). To visualize K18 phosphorylated on serine 53 (P-K18), etoposide-treated SNG-M cells were stained with antibody 3055 that specifically recognizes P-K18 (Liao et al., 1995a). The K18 filament network was stained with antibody 3055 very weakly in most of the nonapoptotic

totic cells. However, a stronger reaction was observed in some cell-cell junctions (Fig. 2 C), consistent with previous results with this antibody (Liao et al., 1995a). Most striking was the bright staining of the K18 granules seen in frankly and presumptive apoptotic cells (Fig. 2, A, C, and E). Cells with only a few reactive granules but with extensive keratin filament bundles were also evident (Fig. 2 A; Fig. 1, A, C, and E). These cells contained normal nuclei, with no sign of fragmentation (Fig. 2 B). Other cells had the K18 cytoskeleton completely reorganized into granules (Fig. 2, C and E). These cells contained abnormal or fragmented nuclei. Thus, P-K18 was preferentially located in the reorganized K18 granules of frankly and presumptive apoptotic cells and at the cell-cell contacts of normal cells.

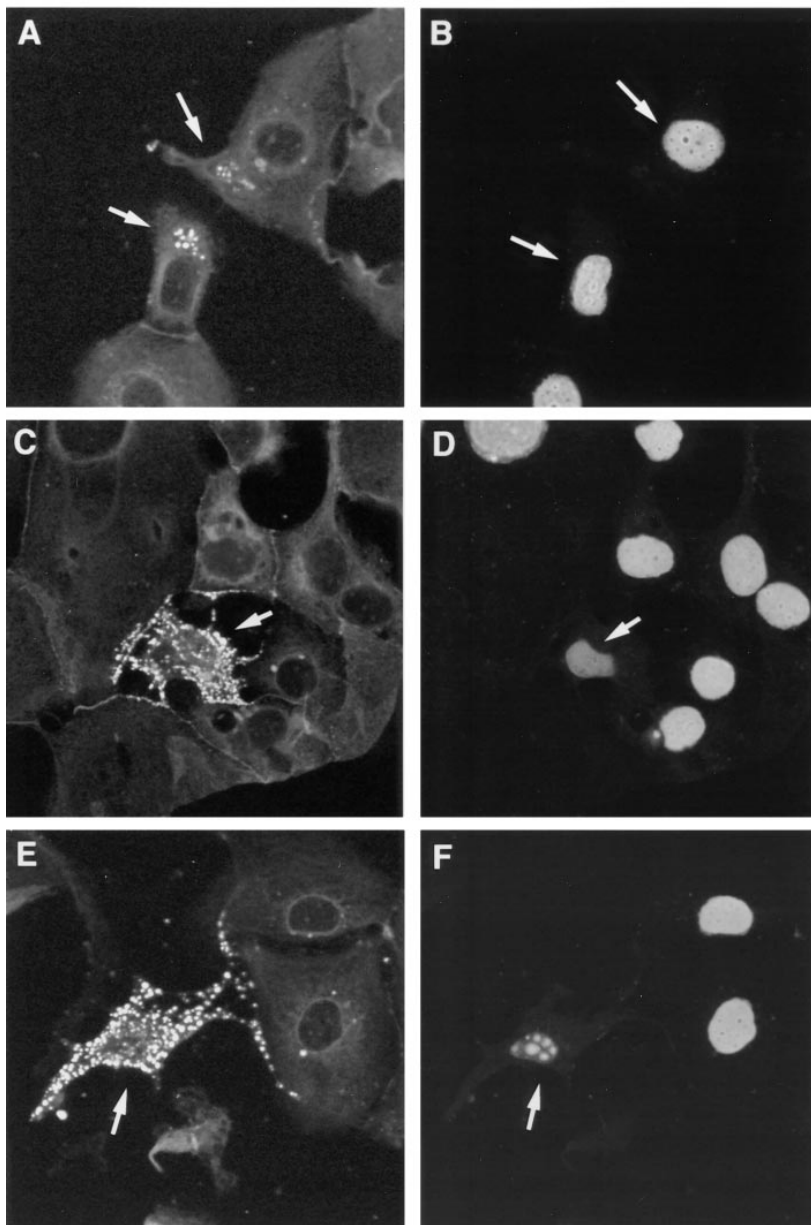


Figure 2. K18 granular structures are preferentially phosphorylated. Etoposide-treated SNG-M cells were fixed and stained by indirect immunofluorescence for phospho-ser53 K18 with antibody 3055 (*A*, *C*, and *E*) and with propidium iodide for DNA (*B*, *D*, and *F*). Note the granular keratin staining of some cells with normal nuclear morphology in *A*, the staining of cell-cell junctions in *A* and *C*, and advanced keratin disorganization with nuclear fragmentation in *C* and *E*.

Specific Cleavage of K18 During Apoptosis

To determine the integrity and phosphorylation state of K18 proteins during apoptosis, we analyzed the K18 protein by Western blotting of SNG-M cells induced to undergo apoptosis by treatment with etoposide. For this purpose, subconfluent cultures of SNG-M cells were incubated with etoposide (250 µg/ml), and adherent and floating cells were collected and combined at different times of etoposide incubation. Whole cell lysates were analyzed by western blotting (Fig. 3). In parallel experiments, typical apoptotic nuclear fragmentation was analyzed by DNA staining with DAPI. Treatment of SNG-M cells with etoposide resulted in progressive induction of apoptosis. After 36 h of treatment, >50% of the cells exhibited apoptotic nuclei. After 60 h, 90% of the cells were apoptotic (Fig. 4 *A*). Western blot analysis showed that etoposide

treatment also resulted in a progressive degradation of K18 and the appearance of a proteolytic product of ~23 kD (Fig. 3 *A*, *K18 B*).

Analysis of K8 expression during etoposide treatment of SNG-M using the same membrane probed with monoclonal antibody M20 showed little change in the amount of K8 during apoptosis (Fig. 3 *C*). By contrast, total K18 degradation was detected with the K18 monoclonal antibody CK5 (Fig. 3 *D*). However, the K18 B fragment was not detected with the CK5 antibody.

To follow the phosphorylation state of K18 during apoptosis, the membrane shown in Fig. 3 *A* was reprobed with antibody 3055, which preferentially recognizes K18 phosphorylated on serine 53 (P-K18) (Fig. 3 *B*). A residual signal for K8 remained on this filter. A careful comparison of the proteins recognized by polyclonal K18 antibody (Fig. 3

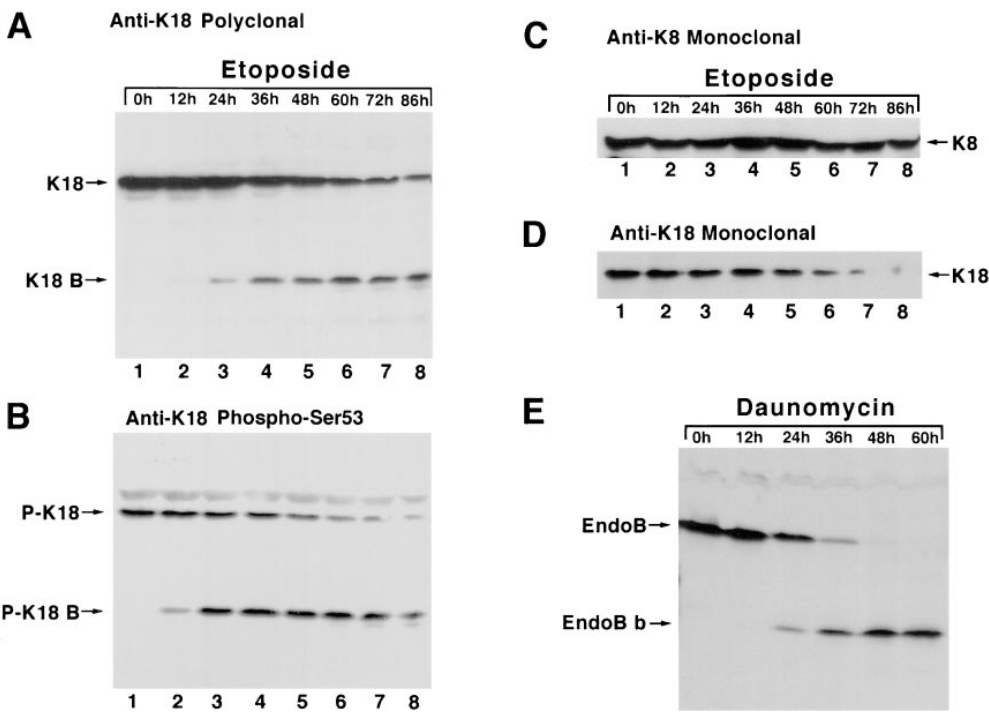


Figure 3. Treatment of SNG-M cells with etoposide results in specific cleavage of K18. (A) SNG-M cells were treated with etoposide (250 µg/ml) for 0, 12, 24, 36, 48, 60, 72, and 84 h. Adherent and floating cells were combined, and whole-cell lysates were analyzed by Western blot with polyclonal antibody anti-K18 1589. This membrane was stripped and probed consecutively with monoclonal anti-K8 M20 (C), anti-phospho ser53-K18 antibodies (B), and monoclonal anti-K18 CK5 (D). (E) HR-9 cells were treated with daunomycin for 0, 12, 24, 36, 48, and 60 h. Adherent and floating cells were combined, and whole-cell lysates were analyzed by Western blot with anti-K18 polyclonal antibody, 1589.

A) and monoclonal K18 (Fig. 3 *D*) confirmed that P-K18 comigrated with K18 (Fig. 3 *B*, lane 1). Importantly, the K18 B fragment found in etoposide-treated SNG-M cells was preferentially recognized by antibody 3055 (Fig. 3 *B*, lanes 2–8). Treatment with etoposide resulted in the progressive disappearance of the full-size P-K18 and the appearance of P-K18 fragment B. This result is interesting in light of the preferential staining of the K18 granules by the P-K18 antibody, 3055, observed in stained cells (Fig. 2). Densitometric analysis of the bands corresponding to K18 in Fig. 3 *A* and P-K18 in Fig. 3 *B* suggests that P-K18 disappeared faster than K18 (Fig. 4 *C*), while the P-K18 B fragment appeared sooner than the K18 B fragment (Fig. 4 *B*). However, the 3055 antibody is more sensitive for the detection of the K18 B fragment than the 1589 polyclonal antibody, which was prepared against the whole mouse K18 protein. The earlier detection of the P-K18 B fragment may be attributed, at least in part, to the greater sensitivity of the 3055 antibody. However, the P-K18 B fragment reached a peak of accumulation earlier than the total K18 B fragment and then declined (Fig. 4 *B*). The decline in the P-K18 B fragment, even while the K18 B fragment continues to increase, suggests that nonphosphorylated K18 can be cleaved. Furthermore, expression of K18 with an alanine substitution for serine 53 in mouse epithelial cells confirmed that phosphorylation of this residue is not required for cleavage during apoptosis (see below). Nevertheless, P-K18 may still be a preferential substrate for cleavage.

Apoptosis was also induced in mouse HR-9 parietal endodermal cells treated with daunomycin. HR-9 treatment with daunomycin resulted in EndoB (mouse K18) cleavage and the appearance of a 24-kD proteolytic fragment (EndoB *b*) (Fig. 3 *E*) after 24 h of treatment. This fragment accumulated in parallel to EndoB disappearance.

After 48 h, almost all the EndoB protein was cleaved to the EndoB *b* fragment.

To study whether K18 cleavage is a generalized event during apoptosis and is preferentially associated with apoptotic cells, we analyzed K18 integrity after the induction of apoptosis using different stimuli in human (SNG-M) and mouse (HR-9) cell lines. Apoptosis was induced by treatment of the cells with etoposide, daunomycin, and UV light. After 24 h of etoposide or daunomycin treatment, or 24 h after brief exposure to UV light, whole cell lysates were prepared from adherent and floating cells and were analyzed by immunoblot analysis using K18 polyclonal antibody (Fig. 5 *A*). Most K18 was present as an intact full-size form in the adherent cells in both HR-9 and SNG-M cells subjected to the different stimuli, whereas floating cells exhibited mainly the K18 proteolytic fragment (Fig. 5 *A*). However, a small amount of cleaved K18 among the total adherent cell population could easily escape detection. Thus, this experiment does not rule out that the granular aggregates detected in a small fraction of adherent SNG-M cells at early times of etoposide treatment by immunofluorescent staining (Fig. 1) contain some cleaved K18. This experiment confirms that different apoptotic stimuli result in similar K18 cleavage in the nonadherent, apoptotic cells.

K18 cleavage was also detected in apoptotic cells of human breast carcinoma MB-231, monkey COS cells, and mouse MT mammary tumor cells (not shown). These results indicate that K18 cleavage is a general characteristic of apoptotic epithelial cells. The K18 cleavage observed in the floating cells is specific for apoptosis and not due to simple detachment of the cells from the plate because no K18 cleavage was detected in log phase cells cultured in suspension for up to 48 h (data not shown).

Apoptosis in the adherent and floating cell populations

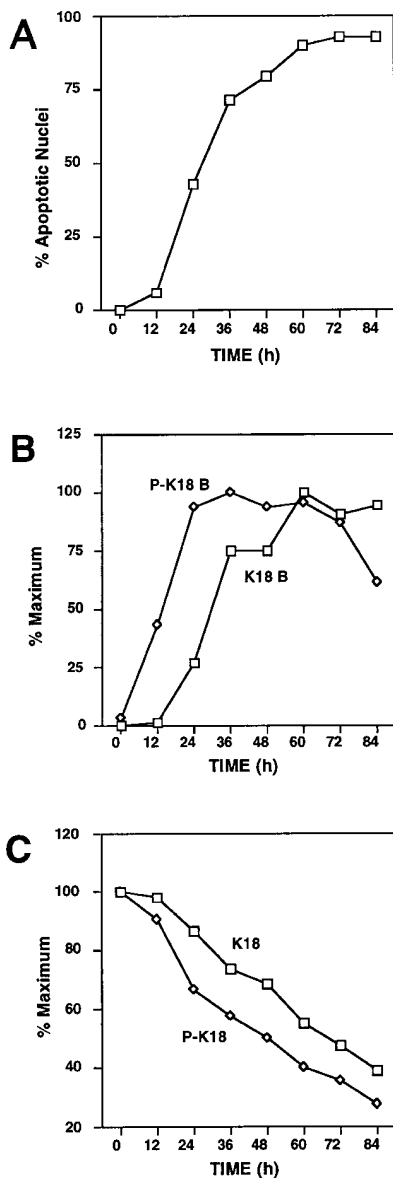


Figure 4. (A) Kinetics of induction of apoptosis in etoposide-treated SNG-M cells. In parallel experiments to the ones described in Fig. 3 A, SNG-M cells were treated with etoposide (250 µg/ml) for 0, 12, 24, 36, 48, 60, 72, and 84 h. Adherent and floating cells were combined, fixed in methanol, and stained with DAPI. Nuclei fragmentation was used as the criterion of apoptosis. (B) Comparison of the kinetics of appearance of the K18 23-kD fragment (K18 B) and its phosphorylated form (P-K18 B) by densitometric analysis of the signal detected in Western blotting shown in Fig. 3, A and B. The y-axis represents the percentage of the maximum signal. Maximum signal for P-K18 B was obtained after 36 h and for K18 B after 60 h. (C) Comparison of the kinetics of disappearance of K18 and P-K18 by densitometric analysis of the signal detected in Fig. 3, A and B.

was confirmed by the analysis of low molecular weight genomic DNA. For every stimulus used for apoptosis, the DNA extracted from the adherent fraction was largely intact (Fig. 5 B, lanes 2, 4, 6, 9, 11, and 13). However, floating cells yielded degraded DNA (Fig. 5 B, lanes 3, 5, 7, 10, 12, and 14) and, in some cases, exhibited the typical DNA ladder. This indicates that the different stimuli resulted in

the production of apoptotic cells in the floating fraction and live cells in the adherent fraction. The nonextractable, high molecular weight DNA of apoptotic cells and of adherent cells migrates very slowly at the top of similar gels (data not shown). These data are consistent with other indicators of apoptosis, such as nuclear morphology and annexin V staining.

Caspases Specifically Cleave K18 In Vitro

Because caspase activation is associated with apoptosis, the K18 cleavage product found in apoptotic cells was compared to isolated K8/K18 incubated in vitro with purified recombinant caspase-6. Human K18 was detected with the 3055 antibody, which reacted very weakly with mouse K18. Purified K18 migrated slightly slower than K18 in whole-cell lysates because of the large difference in total protein load (Fig. 5 C, lanes 1 and 4). When mixed with a whole-cell lysate, isolated K18 comigrated with the cellular K18 (Fig. 5 C, lanes 1 and 3). Purified K18 incubated with caspase-6 resulted in a proteolytic fragment that comigrated with the 23-kD fragment in apoptotic cells (Fig. 5 C, lanes 5 and 7). This result indicated that the K18 B fragment generated in vivo during apoptosis may be the product of caspase cleavage.

To characterize the cleavage of K18 by caspases in more detail, an in vitro cleavage assay was performed with [³⁵S]methionine-labeled K18 and K8 and with purified recombinant caspase-6, -3, and -7. Reticulocyte lysate-translated K8 and K18 were incubated separately with varying amounts of each caspase; the resulting products were analyzed by SDS-PAGE and fluorography. All three caspases specifically cleaved K18 (Fig. 6 A, lanes 7–10, 15–18, and 23–26) but not K8 (Fig. 6 A, lanes 2–5, 11–14, and 19–22) to generate a 23-kD K18 B fragment. Caspase-6 was the most effective because it cleaved at the highest dilution. It also generated fragment C as a major product and, at high caspase concentrations, a trace amount of fragment D (Fig. 6 A, lane 7). Caspase-3 generated primarily fragments B and D and trace amounts of fragment C. The fragment D product is ~19 kD in size (Fig. 6 A, lanes 15–17, fragment D). In addition, caspase-3 but not caspase-6 generated a large fragment that migrated only slightly faster than full-length K18 (Fig. 6 A, lanes 15–18, fragment A). At low concentrations of caspase-3, the A fragment was produced preferentially (Fig. 6 A, lane 18). This pattern of appearance suggests that fragment D may be the product of further digestion of fragment A. Caspase-7 generated a pattern very similar to caspase-3 (Fig. 6 A, lanes 23–26). However, ~100-fold more caspase-7 was necessary to generate an equivalent digestion to caspase-3.

EndoB was also cleaved by the three proteases, resulting in a similar proteolytic pattern as K18, with some difference in the mobility of the fragments (Fig. 6 B, a, b, c, and d). Fragment b had slightly slower electrophoretic mobility than K18 B, whereas c and d displayed faster mobility than C and D, respectively. The differences in mobility from K18 fragments likely reflect small differences in amino acid composition between K18 and EndoB, which is also manifested by the faster mobility for K18, even though it is seven residues larger than EndoB (Fig. 6 B, lanes 1 and 5) (Oshima et al., 1986).

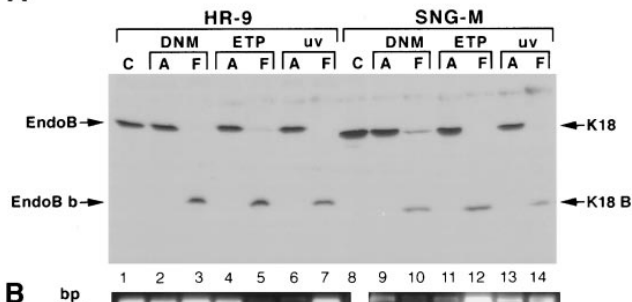
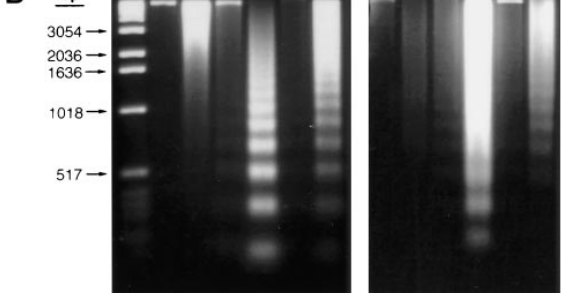
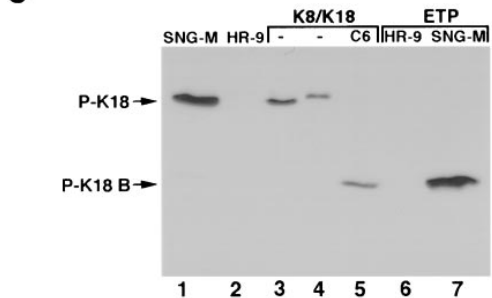
A**B****C**

Figure 5. Different apoptotic stimuli results in the cleavage of K18 and EndoB. (A) Western blot analysis of HR-9 (lanes 1–7) and SNG-M (lanes 8–14) cells subjected to different apoptotic stimuli. Adherent (A) and floating (F) cells were separately collected after etoposide (ETP) and daunomycin (DNM) treatment and UV exposure, and whole-cell lysates were analyzed by Western blot with polyclonal anti-K18. Lanes 1 and 9 represent control untreated cells. (B) Low molecular weight genomic DNA was analyzed from cells represented in A except for lane 1, which contained size markers. (C) Comparison of K18 found in apoptotic cells and purified K18 cleaved in vitro by caspase-6. Cell lysates or purified protein preparation was analyzed by Western blotting with antibody 3055. Untreated SNG-M cells (lane 1), etoposide (ETP) treated floating SNG-M cells (lane 7), and mouse HR-9 cells (lane 2) or apoptotic HR-9 cells (lane 6) were compared with purified K18 (lane 4), purified K18 mixed with HR-9 cell lysate (lane 3), or K18 cleaved with caspase-6 (C6) in vitro and mixed with HR-9 cell lysate (lane 5). Note the comigration of caspase-6-cleaved K18 (lane 5) and K18 B found in apoptotic SNG-M cells (lane 7).

Mapping of the Cleavage Sites

K18 cleavage by caspases-3, -6, and -7 all generated the B proteolytic fragment found in apoptotic epithelial cells. In addition, caspases-3 and -7 also preferentially cleaved K18 to generate the A fragment with a slightly faster mobility than K18. To map the location of both cleavage sites, COOH-terminal deletions of the K18 and EndoB proteins

were generated by transcribing and translating the cDNAs truncated within the coding regions at several different restriction enzyme sites (Fig. 7, A and C). Translation of these truncated mRNAs resulted in K18 proteins of 339 residues (K18-339) and 269 residues (K18-269), instead of the full-length 430 amino acids. These truncated forms of K18 were cleaved with caspases-6, -3, and -7 to analyze the proteolytic profile generated. Cleavage of K18-339 with caspases-3 and -7 (Fig. 7 B, lanes 7 and 8) did not produce any slightly smaller fragment that might correspond to fragment A of the full-length protein. Thus, the cleavage site of caspases-3 and -7 that generates the A fragment likely resides between residue 339 and the COOH-terminal end. All three caspases generated the B fragment from both K18-339 and K18-269. Thus, the B fragment originates from the NH₂-terminal half of K18, from the cleavage just upstream of residue 269 (Fig. 7 B, lanes 10 and 11). If one caspase-6 site is responsible for the generation of the B and C fragments from wild-type K18, a severely truncated C fragment might be expected by digestion of K18-339. However, this fragment was not detected, perhaps because it may migrate near the buffer front with the excess free, radioactive methionine.

The same approach was used to map the cleavage sites for caspases in EndoB. Three deletion mutants of EndoB in the COOH-terminal were generated and cleaved with the different caspases. The full-length EndoB is 423 residues. Truncation of the EndoB cDNA with AvaI, ScaI, and PvuII generated proteins of 316, 262, and 191 residues, respectively (Fig. 7 C). Cleavage of EndoB-316 with caspases-6, -3, and -7 (Fig. 7 D, lanes 6–8) produced the b fragment without any indication of an a fragment derivative. Thus, as for K18, the site that generates the a fragment must have been deleted in EndoB-316. EndoB-262 is slightly larger than the b fragment, and the cleavage with all three caspases still generated the b fragment (Fig. 7 D, lanes 10–12), indicating that the cleavage site that generates the b fragment is upstream but close to amino acid 262. This places the site close to the conserved VEVD/A sequence also found in the K18 protein (Fig. 7, A and C). EndoB-191 is smaller than the b fragment, and no site of cleavage for any of the caspases was found in the first 191 residues of the protein.

Mutagenesis of the K18 Caspase Cleavage Site

Caspases are considered to require an aspartic acid residue at the P1 position immediately upstream of the cleavage site for efficient cleavage. To assess whether the VEVD238 sequence in the linker region of K18 is the target for caspases, we mutated the aspartate to glutamate. A [³⁵S]methionine-labeled K18 mutant protein (K18-D238E) was synthesized by coupled transcription and translation. The sensitivity of this protein to digestion by caspases-3 and -6 was compared to wild-type K18. Caspase-3 cleaved K18 in a time-dependent manner generating the A, B, and D fragments as expected (Fig. 8 A, lanes 1–7). By contrast, K18-D238E produced only the A fragment, while the B and D fragments were absent (Fig. 8 A, lanes 8–14). Thus, changing the aspartate to a glutamate in the sequence VEVD appears to abolish the internal cleavage but not the COOH-terminal domain digestion. The mutant K18-

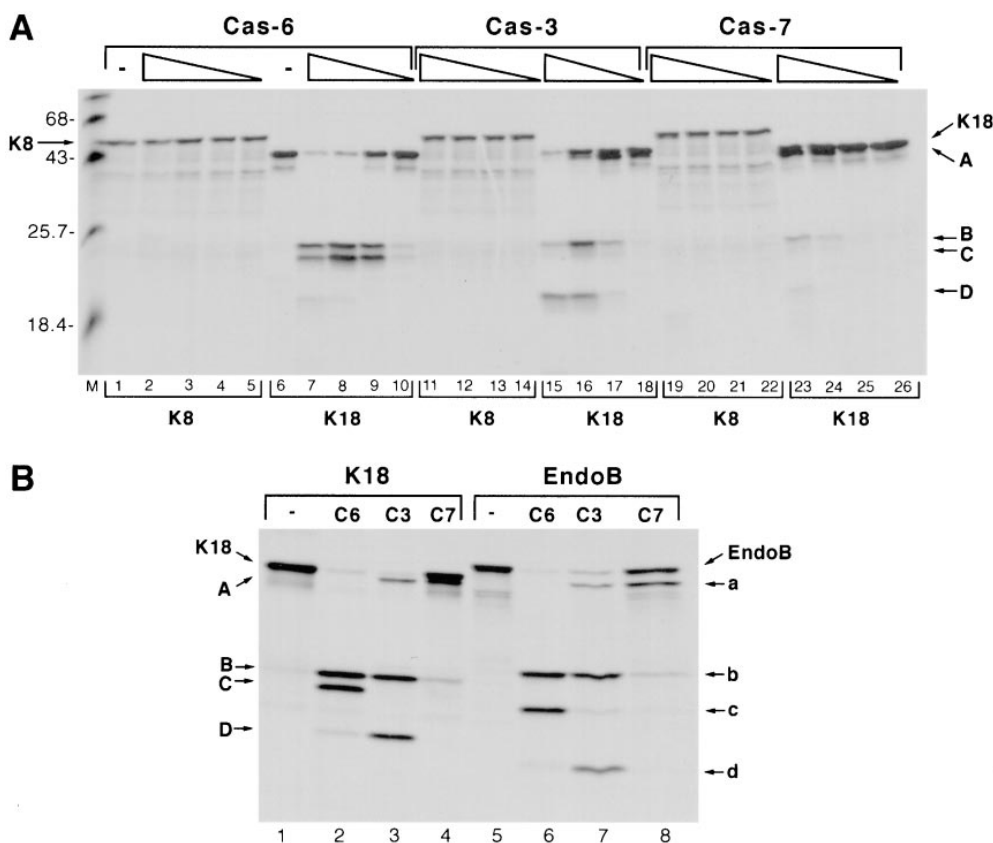


Figure 6. Specific cleavage in vitro of K18, but not K8, by caspase-6, -3, and -7. (A) [35 S]methionine-labeled K8 and K18 were incubated for 2 h at 37°C with decreasing concentrations of caspase-6 (Cas-6) (lanes 2–10), caspase-3 (Cas-3) (lanes 11–18), and caspase-7 (Cas-7) (lanes 19–26), and subsequently analyzed by SDS-PAGE and fluorography. Protease was decreased by serial 1:10 dilutions. (B) Comparison of the proteolytic pattern of K18 and EndoB cleavage generated by caspase-6 (C6), caspase-3 (C3), and caspase-7 (C7). A–D represent the proteolytic fragments obtained by cleavage of K18. a–d represent the proteolytic fragments obtained by cleavage of EndoB.

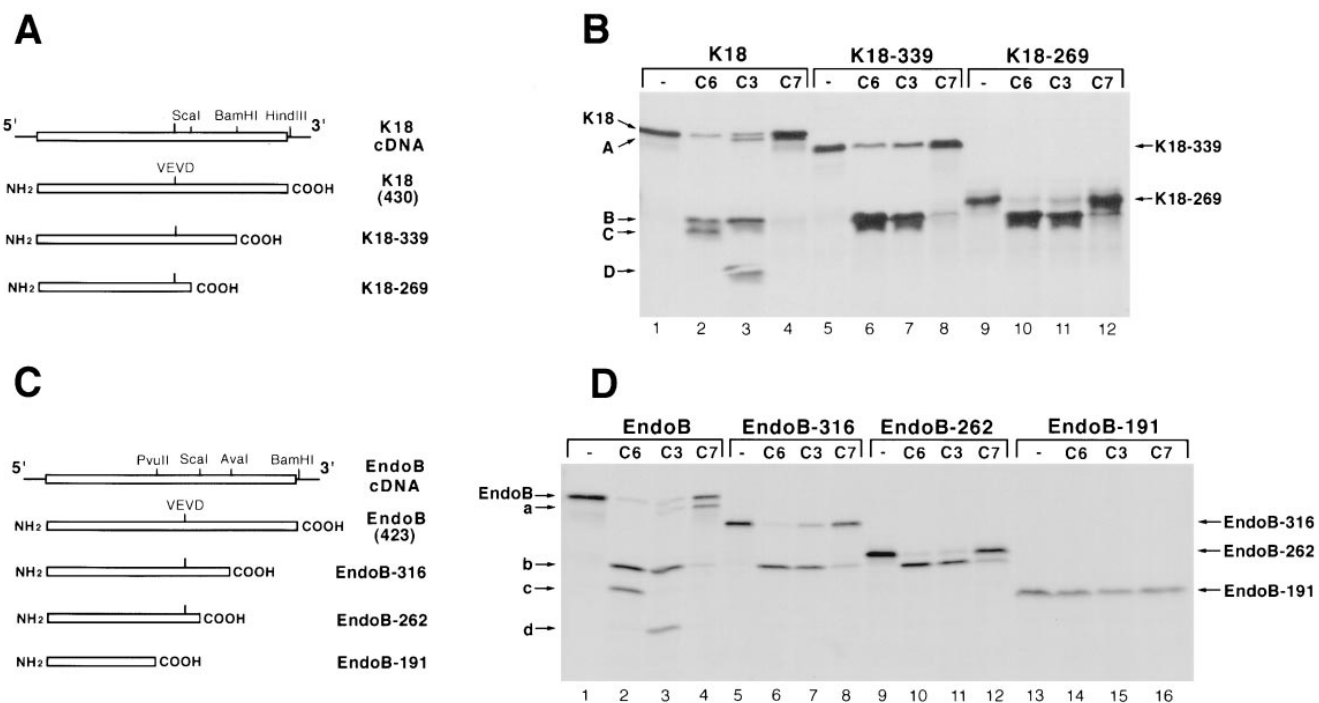


Figure 7. Mapping of the caspase cleavage sites for K18 and EndoB. (A) Schematic representation of the deletion mutants of K18 obtained by in vitro transcription and translation of K18 cDNA digested with HindIII (K18), BamHI (K18-339), and ScaI (K18-269). (B) [35 S]methionine-labeled K18 and K18 mutants were separately incubated for 2 h at 37°C with caspase-6 (C6), caspase-3 (C3), and caspase-7 (C7) and subsequently analyzed by SDS-PAGE and fluorography. (C) Schematic representation of the deletion mutants of EndoB obtained by in vitro transcription and translation of EndoB cDNA digested with BamHI (EndoB), Avai (EndoB-316), ScaI (EndoB-262), and PvuII (EndoB-191). (D) [35 S]methionine-labeled EndoB and EndoB mutants were separately incubated for 2 h at 37°C with caspase-6 (C6), caspase-3 (C3), and caspase-7 (C7) and subsequently analyzed by SDS-PAGE and fluorography.

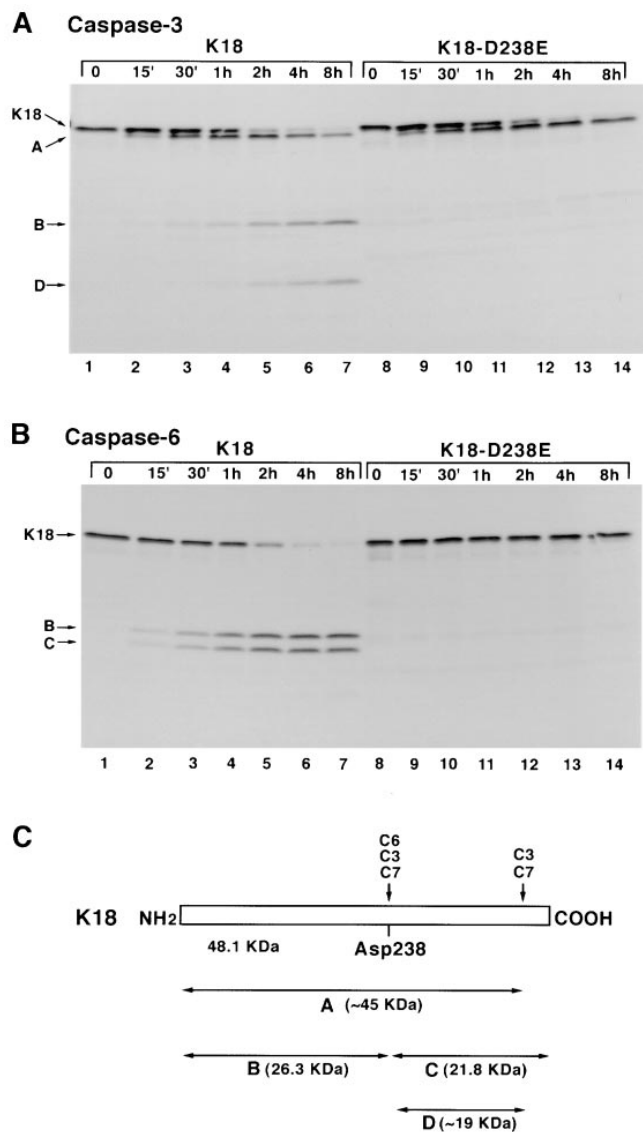


Figure 8. Site-directed mutagenesis to K18-D238E abolishes cleavage by caspases. (A) Time-dependent cleavage of K18 and K18-D238E with caspase-3. Equal amounts of [³⁵S]methionine-labeled K18 and K18-D238E were incubated with caspase-3. The reaction was stopped at 0, 15 min, 30 min, 1 h, 2 h, 4 h, and 8 h, and samples were analyzed by SDS-PAGE and fluorography. (B) Time-dependent cleavage of K18 and K18-D238E with caspase-6. Equal amounts of [³⁵S]methionine-labeled K18 and K18-D238E were incubated with caspase-6. The reaction was stopped at the indicated times, and samples were analyzed by SDS-PAGE and fluorography. (C) Schematic representation of the different proteolytic fragments generated by cleavage of K18 by caspases.

D238E protein was also resistant to caspase-6 digestion (Fig. 8 B). In this case, caspase-6 does not cleave the COOH-terminal domain site recognized by caspase-3 and -7.

The identification of the VEVD/A sequence in K18 as the target of caspase digestion provides the information necessary to interpret the origin of all four fragments generated by the different caspases (Fig. 8 C). Digestion of K18 with caspase-6 generated the B, NH₂-terminal fragment of 238 residues with a molecular mass of 26.3 kDa.

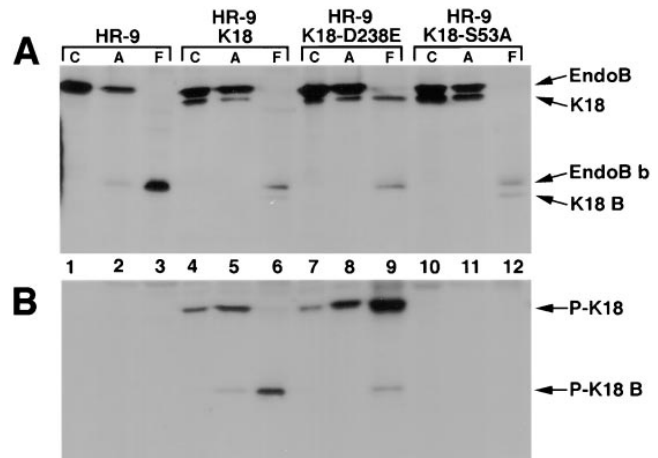


Figure 9. Western blot analysis of K18, K18-D238E, and K18-S53A proteins expressed in HR-9 normal and apoptotic cells. (A) Whole cell lysates of stably transfected HR-9 cells expressing the indicated proteins were prepared from control cultures (C) and after treatment with daunomycin for 24 h. Attached cells (A) and floating cells (F) were analyzed separately. After SDS-PAGE and transfer to nitrocellulose, the proteins were probed with the 1589 polyclonal EndoB antibody. (B) The same filter was re-probed with 3055 polyclonal antibody specific for K18 phosphorylated on ser53.

The estimated size of the B fragment was 23 kDa from gel mobility. These values appear within reasonable agreement, considering the slightly anomalous migration behavior of K18. The C fragment is predicted to be 192 residues with a molecular mass of 21.8 kDa, which is very close to the value of 22 kDa estimated from the gels. The exact location of the COOH-terminal cleavage site, which generates fragments A and D by caspase-3 and -7, is not known. However, the difference between fragments C and D is ~3 kDa, which would place the site at the COOH-terminal, non- α helical tail domain.

Expression of K18-D238E and K18-S53A in Epithelial Cells

To determine the importance of the primary K18 caspase cleavage site and the phosphorylation of ser53 for K18 cleavage in cells during apoptosis, HR-9 mouse parietal endodermal cells were transfected with expression constructs for the wild-type K18, the ser53→ala (K18-S53A) and the asp238→glu (K18-D238E) mutant forms of K18, and isolated clones that persistently expressed the human protein. The human forms of K18 could be distinguished from the endogenous mouse K18 (EndoB) by the CK5 monoclonal antibody, the 3055 antiserum, and differences in mobility in SDS-PAGE. Representative clones with the highest proportion of CK5-positive cells were examined further.

Apoptosis was induced by treatment with daunomycin, and after 24 h, cell lysates were prepared from adherent and floating cells and were analyzed by Western blot with polyclonal antibody 1589, which recognizes both K18 and EndoB. As expected, most of the EndoB present in the adherent population is the full-length EndoB (Fig. 9 A,

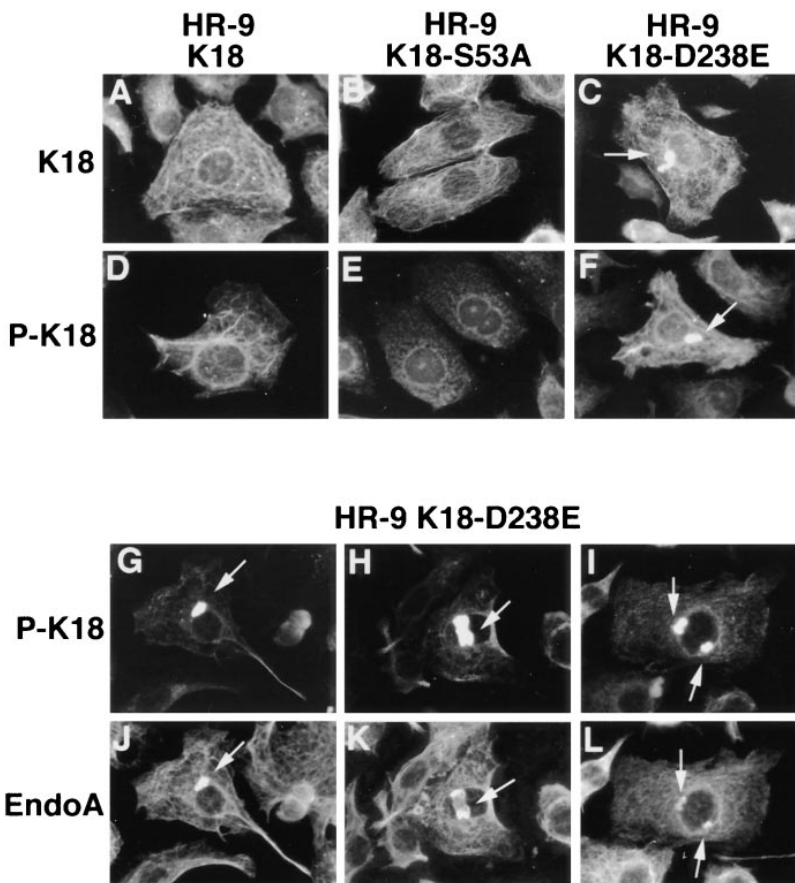


Figure 10. Immunofluorescent localization of K18, P-K18, and EndoA in HR-9 cells expressing K18 (A and D), K18-S53A (B and E) or K18-D238E (C and F-L). Cells were stained for K18 with CK5 monoclonal antibody (A-C) and with 3055 antibody for P-K18 (D-F). Note the presence of keratin aggregates (arrows) that are preferentially phosphorylated in HR-9 K18-D238E cells. Double staining of HR-9 K18-D238E cells with 3055 antibody (G-I) and monoclonal antibody anti-EndoA TROMA1 (J-L) show colocalization of EndoA with P-K18 in the granular structures.

lane 2), whereas the floating fraction contains mainly the proteolytic fragment, EndoB *b* (Fig. 9 A, lane 3). K18-transfected HR-9 cells express both K18 and EndoB (Fig. 9 A, lane 4), and both remain in the adherent cells after treatment with daunomycin (Fig. 9 A, lane 5). However, EndoB and K18 disappeared in the floating cells to generate the proteolytic fragments EndoB *b* and K18 B (Fig. 9 A, lane 6), indicating that both endogenous EndoB and exogenous K18 are cleaved in apoptotic HR-9 cells. K18-D238E is also present in the adherent population of transfected HR-9 cells (Fig. 9 A, lane 8) along with EndoB. However, whereas EndoB disappears in the floating fraction, K18-D238E still remains (Fig. 9 A, lane 9), showing resistance to cleavage. This result is consistent with use of the caspase cleavage site VEVD/A in vivo. A small amount of K18-D238E cleavage product is detected when the 3055 antibody is used (Fig. 9 B, lane 9), indicating that this conservative mutation dramatically decreases the sensitivity of K18 to cleavage but does not completely abolish it in cells. Nevertheless, the high level of full-length K18-D238E in nonadherent, apoptotic HR-9 differs dramatically from the behavior of wild-type K18, EndoB, or K18-S53A (see below) and confirms that the primary caspase cleavage site identified in vitro is also used in cells.

Induction of apoptosis in HR-9 cells transfected with K18-S53A resulted in the cleavage of both EndoB and K18-S53A in the floating cells (Fig. 9 A, lane 12), indicating that phosphorylation of ser53 is not required for the caspase cleavage of K18, at least within the context of endogenous wild-type EndoB. Absence of phosphorylation

in K18-S53A was confirmed by Western blot with antibody 3055 (Fig. 9 B, lanes 10–12).

Keratin Filament Organization of K18-S53A and K18-D238E

Transient expression of wild-type K18, K18-S53A, and K18-D238E all resulted in cells that appeared to incorporate the human K18 proteins into the endogenous keratin network of HR-9 cells without significant perturbations (data not shown). HR-9 cells that continued to express either wild-type K18 or K18-S53A after drug selection were isolated and stained with the CK5 monoclonal antibody or the 3055 antibody to visualize K18 and P-K18. Both K18 and K18-S53A were found in the endogenous mouse keratin filament system (Fig. 10, A and B, antibody 1589 staining not shown). Some of the cells expressing wild-type K18 contained detectable P-K18 in a filamentous organization (Fig. 10 D), although in most cells the staining was quite weak. As expected, no specific staining of K18-S53A was detected by the 3055 antibody (Fig. 10 E). Only background staining, equivalent to that produced by the secondary antibody or by cells that ceased K18 expression, was detected (Fig. 10 F, bottom left).

Cells stably transfected with K18-D238E grew slowly, generated aberrant large cells, and appeared to be selected for the loss of expression because the proportion of cells that stained with CK5 antibody decreased as the culture expanded. The resulting population contained only ~30% K18-positive cells in the best clone. Multiple additional

clones failed to sustain detectable K18-D238E expression. Immunofluorescent staining revealed positive cells with aggregates of keratin filaments in an altered organization (Fig. 10 C) as well as protein distributed in a filamentous organization. The nuclei of these cells did not have alterations associated with apoptosis, and Western blotting confirmed the absence of detectable cleavage of EndoB in growing cultures (Fig. 9 A, lane 7). Thus, this aggregation was not due to induction of apoptosis. These aggregates were preferentially reactive with the 3055 antibody specific for P-K18 (Fig. 10, F–J). The remaining filamentous K18-D238E (Fig. 10 C) reacted very weakly with the 3055 antibody. In addition, the 3055 antibody permitted the double staining for the mouse complementary type II keratin, EndoA, with a monoclonal antibody. EndoA was colocalized in the aggregates (Fig. 10, J–L) as well as in a filamentous organization in the same cell. The aggregates of P-K18-D238E and EndoA were commonly localized at the edge of the nucleus.

Comparison of the amounts of K18-D238E and K18-S53A by immunoblotting suggests that K18-D238E is not expressed at an excessively high level per cell, even after normalizing for the percentage of K18-positive cells (100% for HR-9 K18S53A and ~30% for HR-9 K18-D238E). These results suggest that the K18-D238E protein may act as a subtle dominant negative mutant. The presence of normal-appearing keratin organization in some of both the stably transfected cells and all the transiently transfected cells suggests that this effect may be more subtle than many dominant negative acting mutants of keratins (Kulesh et al., 1989; Ku et al., 1995). It is possible that the cleavage of K18 by caspases may play some role in the normal metabolism of K18 filaments as well as during apoptosis. Such an effect may only be manifest after cell division. However, it is well known that the level of expression of dominant negative-acting intermediate filament proteins can greatly influence the appearance of the keratin filament network (Kulesh et al., 1989). K18-D238E was expressed from an expression vector different than the other two forms of K18. However, we have successfully expressed K8 with a very similar expression vector in epithelial cells without observing similar aggregates (Oshima, R.G., and H. Baribault, unpublished observations). Thus, we would suggest that K18-D238E behaves significantly differently than K18 or K18-S53A within mouse epithelial cells. Cleavage of K18-D238E was inhibited in apoptotic cells, thus confirming the importance of the site during programmed cell death.

Discussion

We have explored the fate of keratin intermediate filament proteins in apoptotic epithelial cells and have discovered that a dramatic reorganization of the keratin cytoskeleton precedes morphological nuclear disruption during apoptosis and is associated with the phosphorylation of K18 on serine 53. Degradation of simple epithelial keratins involves the specific cleavage of K18, but not K8, in a conserved non- α helical linker region by caspase proteins. The caspase recognition sequence in K18 is identical to that found in lamin B and is conserved in multiple other IF family members. This suggests that the process of caspase

degradation of K18 in several types of epithelial cells may reflect a general model of initiation of IF processing during apoptosis.

After the initiation of the process of apoptosis in epithelial cells, but before obvious nuclear degeneration, keratin filaments begin to reorganize, first locally and then globally throughout the cell into discrete granular structures. Disorganized keratin filaments in frankly apoptotic cells has been previously reported (Machiels et al., 1996). We have found that this reorganization preferentially involves K18 phosphorylated on serine 53. K18 phosphorylated on serine 53 may be a preferential substrate for proteolytic cleavage resulting in the diagnostic 26.3-kD fragment derived from the NH₂-terminal half of K18. However, the cleavage of K18-S53A expressed in apoptotic HR-9 cells shows that it is not strictly required. Caspases, which are activated during apoptosis, digest K18 at the sequence VEVD/A located within the non- α helical L1-2 linker region.

While treatment of the SNG-M epithelial cells with etoposide resulted in a dramatic change in the organization of the K8/K18 IF into granular structures, it is not clear whether this reorganization is due only to the phosphorylation of K18, its proteolytic cleavage, or both. One technical complication to the resolution of this question is that epithelial cells undergoing apoptosis detach from the substrate and the degree and speed of this detachment varies in different cell types (data not shown). Also no reagents are currently available to specifically identify cleaved K18 within the apoptotic cells that remain attached. However, it is well known that phosphorylation is involved in the regulation of the polymerization state of keratin filaments during other normal cell processes (Franke et al., 1982; Klymkowsky et al., 1991; Liao et al., 1995a; Ku et al., 1996a; Toivola et al., 1997) and of other intermediate filaments as well (Inagaki et al., 1997). Different stress conditions, such as rotavirus infection and heat shock stress, can provoke reorganization of K8/K18 IF in a process that correlates with an increase in the phosphorylation and solubility of K8 and K18 (Liao et al., 1995b). Further evidence that phosphorylation may alter the polymerization state of K8 and K18 filaments is the rapid effect of the phosphatase inhibitor, microcystin LR, on isolated hepatocytes (Toivola et al., 1997). In addition, these investigators detected a protein of about the same size as the K18 B fragment in immunoprecipitates of toxin-treated hepatocytes, which suggestss that microcystin LR may initiate a rapid apoptotic program. Furthermore, the K18-D238E mutant protein is clearly capable of being phosphorylated on serine 53 (Figs. 9 and 10). Together, the available data would be consistent with phosphorylation of K18 being a parallel process rather than a concerted step in a pathway leading to cleavage.

The decrease in K18 during the period of drug treatment is in contrast to the apparent stability of K8. While this is consistent with the resistance of K8 to cleavage by caspases, the fate of K8 remains to be determined. K8 is colocalized with K18 in the keratin aggregates (data not shown). Previous studies have shown that either K8 or K18 that is expressed in excess of a stabilizing partner is degraded rapidly (Kulesh et al., 1989). Furthermore the destabilization of keratin filaments by the overexpression

of truncated or mutant forms of several different keratins results in reorganization, or collapse, of the cellular keratin filament network and the formation of granular structures (Albers and Fuchs, 1989; Kulesh et al., 1989; Couloomb et al., 1990). It is possible that limited proteolytic cleavage may participate in the reorganization of the filament networks in apoptotic epithelial cells. Cleavage of K18 has also been reported in HeLa cells infected with adenovirus. In these cells, cleavage of the amino-terminal end of K18 by the adenovirus L3 23-kD proteinase results in reorganization of the K18 IF into spheroid globules (Chen et al., 1993).

Caspases are considered essential to the execution of apoptosis by a variety of stimuli. Inhibition of caspase activity, by naturally occurring inhibitors such as the baculovirus product p35 (Bump et al., 1995; Xue and Horvitz, 1995) or by synthetic inhibitors, blocks apoptosis in multiple systems (Clem et al., 1991; Rabizadeh et al., 1993; Sugimoto et al., 1994). The comigration of the apoptotic-dependent K18 B fragment with the NH₂-terminal fragment of K18 generated by caspases-3, -6, and -7 is consistent with the view that a caspase is responsible for the generation of the K18 B fragment in apoptotic epithelial cells. This is supported by the resistance of K18-D238E to cleavage in transfected apoptotic HR-9 cells. Furthermore, evidence that endogenous K18 is cleaved at the caspase recognition site during the drug-induced apoptosis of HT29 human colonic tumor cells has been obtained by another laboratory by direct protein sequencing of the K18 22- and 26-kD fragments (Bishr Omary, personal communication). All current evidence is consistent with a caspase digestion of K18 as responsible for the K18 B fragment. While the large K18 A fragment generated by both caspases-3 and -7 was not detected in apoptotic human cells or mouse HR-9 cells expressing K18, this cleavage may be masked under normal conditions by other subsequent steps in the degradation of keratin filaments. Thus, it is not possible to deduce the identity of the caspases responsible for K18 cleavage during apoptosis based on the cleavage products alone. However, it is of interest that all three caspases cleave the VEVD/A sequence but that caspase-6 is the most effective. This is consistent with the known extended specificity of caspase-6, which prefers aliphatic side chains at the P4 position, compared with caspases-3 and -7, which prefer acidic side chains here. The K18 COOH-terminal site cleaved by caspases-3 and -7 is not known but may be at DALD/S398, as this would be better recognized by these caspases than by caspase-6. Furthermore, this cleavage site would generate a fragment of 3.4 kD that is close to our estimated difference in size between the C and D fragments.

Caspase-3 can cleave K18 but not lamins A and C, which contain the sequence VEID (Takahashi et al., 1996). The VEVD sequence is also the cleavage site for lamin B1 and B2 (Rao et al., 1996). A comparison of the L1-2 linker region of other IF proteins (Fig. 11) reveals that the VEVD sequence is also found in K19 and K20, thus prompting the prediction that these type I keratins would also be substrates for caspases. Furthermore, the sequence VEMD is found at the same position in K13, K14, K15, K16, K17, desmin, and NF-L. Thus, all of the type I keratins with the exception of K9 and K10 are potential

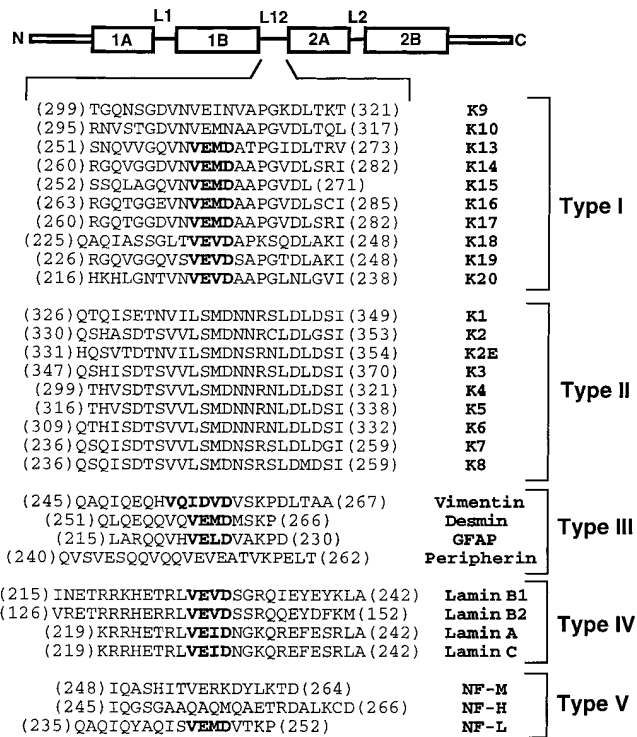


Figure 11. Amino acid sequences of the linker L1-2 region of the central rod domain of the different members of the IF family. Potential caspase cleavage sites are highlighted. Sequences were obtained from Swiss-Prot database.

substrates for caspase digestion, although not necessarily the same caspases as are active on K18. K9 and K10 are expressed in suprabasal layers of stratified squamous epithelia in cells that are committed to terminal differentiation, which includes cell death and culminates with the production of nucleated squames highly enriched in keratin. The absence of the caspase cleavage sites in K9 and K10 may reflect their extracellular, structural function.

It is interesting that mutations of the V and A of the sequence VEMD/A have been detected in the K14 gene of patients with the Weber-Cockayne form of epidermolysis bullosa simplex (EBS), a genetic blistering skin disease (Rugg et al., 1993; Fuchs, 1997). Furthermore, the mutations of this region result in very subtle or no apparent differences in the polymerization of purified mutant proteins in vitro or the appearance of keratin filaments within cells. In this respect, K18-D238E may prove to behave in a similar fashion. This conservative change may result in subtle structural abnormalities of K8 and K18 filaments that ultimately result in the disruption of keratin filament organization, perhaps only reflected in polymerization states of higher order than 10-nm filaments or after cell division. However, it is also possible that both K18-D238E and the K14 mutations of the VEMD/A site may reflect a previously unrecognized requirement for partial caspase cleavage of type I keratin proteins in nonapoptotic cells. Some caspases, like caspase-1 (interleukin-converting enzyme), do have functions other than in apoptosis. Furthermore,

caspase-3 activation has been demonstrated in cell processes independent of cell death (Miossec et al., 1997).

The proteolytic cleavage of K18 is of particular interest from a clinical perspective because elevated levels of fragments of K18 are found in the serum of patients with a variety of carcinomas (Weber et al., 1984; Bonfrer et al., 1994; Einarsson, 1995). The purification of tissue polypeptide-specific antigens include a 22-kD K18 fragment (Rydlander et al., 1996), which may correspond to the K18 C fragment. Additional reports of the detection of K8 on the external surfaces of some cells (Hembrough et al., 1995) may be related to the competition between apoptotic and necrotic death of cells, which could result in the exposure of keratin proteins or fragments to the external milieu and the circulation.

Is the degradation of K18 of functional significance to the apoptotic process? We expected that HR-9 cells that express K18-D238E might be useful to explore this question. While it is clear that the expression of K18-D238E certainly does not prevent apoptosis of mouse HR-9 cells, a moderate effect was difficult to evaluate because of the poor growth and mosaic expression that appears to accompany the forced expression of the mutant protein. In addition, HR-9 cells detach early in the apoptotic process. We were thus unable to determine the impact of either K18-S53A or K18-D238E on the type of apoptotic keratin granule organization found in SNG-M cells. A careful comparison of the kinetics of cell death induced by different stimuli or the inducible expression of the K18-D238E protein may help address this question in the future. K8/K18 filaments are essential for normal development (Baribault et al., 1993). However, in certain genetic backgrounds, some mice lacking K8 (and also K18 because of degradation in organs that lack another complementary type II keratin) survive to adulthood. These animals are more sensitive to drugs such as griseofulvin and partial hepatectomy and develop colorectal hyperplasia (Baribault et al., 1994; Oshima et al., 1996). Apoptosis may be a common process among these different characteristics. Furthermore, there are several reports that link K8 and K18 expression with either drug resistance or sensitivity (Bauman et al., 1994; Parekh and Simpkins, 1995; Anderson et al., 1996). Thus, while there is as of yet no compelling evidence of the participation of K18 filaments directly in modulating apoptosis, the recent development of mice and epithelial cell lines with keratin null alleles and various keratin mutations may provide the opportunity to determine the functional role, if any, of simple epithelial keratins in programmed cell death.

We are grateful to Bishr Omary (VA Hospital and Stanford Medical School, Palo Alto, CA) for stimulating and open discussions, gifts of the 3055 polyclonal antibody, K8 and K18 proteins, the pGC1853-K18S15A plasmid, and personal communication regarding protein sequencing results of the 26- and 22-kD fragments observed in apoptotic HT-29 cells before publication.

This work was supported by grants from the National Institutes of Health, to R.G. Oshima (5 R01 CA42302) and to G. Salvesen (5 R01 HL51399), and from a Cancer Center support grant (P30 CA30199). Caulín was supported in part by a postdoctoral fellowship from the Spanish Ministry of Education and Science.

Received for publication 24 March 1997 and in revised form 11 July 1997.

References

- Albers, K., and E. Fuchs. 1989. Expression of mutant keratin cDNAs in epithelial cells reveals possible mechanisms for initiation and assembly of intermediate filaments. *J. Cell Biol.* 108:1477–1493.
- Alnemri, E.S., D.J. Livingston, D.W. Nicholson, G. Salvesen, N.A. Thornberry, W.W. Wong, and J. Yuan. 1996. Human ICE/CED-3 protease nomenclature. *Cell* 87:171.
- Anderson, J.M., L.M. Heindl, P.A. Bauman, C.W. Ludi, W.S. Dalton, and A.E. Cress. 1996. Cytokeratin expression results in a drug-resistant phenotype to six different chemotherapeutic agents. *Clin. Cancer Res.* 2:97–105.
- Baribault, H., J. Price, K. Miyai, and R.G. Oshima. 1993. Mid-gestational lethality in mice lacking keratin 8. *Genes Dev.* 7:1191–1202.
- Baribault, H., J. Penner, R.V. Iozzo, and M. Wilson-Heiner. 1994. Colorectal hyperplasia and inflammation in keratin 8-deficient FVB/N mice. *Genes Dev.* 8:2964–2973.
- Bauman, P.A., W.S. Dalton, J.M. Anderson, and A.E. Cress. 1994. Expression of cytokeratin confers multiple drug resistance. *Proc. Natl. Acad. Sci. USA.* 91:5311–5314.
- Bonfrer, J.M.G., E.M. Groeneveld, C.M. Korse, A. Van Dalen, L.C.J.M. Oomen, and D. Ivanyi. 1994. Monoclonal antibody M3 used in tissue polypeptide-specific antigen assay for the quantification of tissue polypeptide antigen recognizes keratin 18. *Tumor Biol.* 15:210–222.
- Brancolini, C., M. Benedetti, and C. Schneider. 1995. Microfilament reorganization during apoptosis: the role of Gas2, a possible substrate for ICE-like proteases. *EMBO (Eur. Mol. Biol. Organ.) J.* 14:5179–5190.
- Brulet, P., C. Babinec, R. Kemler, and F. Jacob. 1980. Monoclonal antibodies against trophoblast-specific markers during mouse blastocyst formation. *Proc. Natl. Acad. Sci. USA.* 77:4113–4117.
- Bump, N.J., M. Hackett, M. Hugunin, S. Seshagiri, K. Brady, P. Chen, C. Ferenz, S. Franklin, T. Ghayur, P. Li, et al. 1995. Inhibition of ICE family of proteases by baculovirus antiapoptotic protein p35. *Science (Wash. DC)*. 269:1885–1888.
- Casciola-Rosen, L.A., D.K. Miller, G.J. Anhalt, and A. Rosen. 1994. Specific cleavage of the 70-kDa protein component of the U1 small nuclear ribonucleoprotein is a characteristic biochemical feature of apoptotic cell death. *J. Biol. Chem.* 269:30757–30760.
- Chen, P.H., D.A. Ornelles, and T. Shenk. 1993. The adenovirus L3 23-kilodalton proteinase cleaves the amino-terminal head domain from cytokeratin 18 and disrupts the cytokeratin network of HeLa cells. *J. Virol.* 67:3507–3514.
- Chu, Y.W., R.B. Runyan, R.G. Oshima, and M.J.C. Hendrix. 1993. Expression of complete keratin filaments in mouse L cells augments cell migration and invasion. *Proc. Natl. Acad. Sci. USA.* 90:4261–4265.
- Chu, Y.W., E.A. Seftor, L.H. Romer, and M.J.C. Hendrix. 1996. Experimental coexpression of vimentin and keratin intermediate filaments in human melanoma cells augments motility. *Am. J. Pathol.* 148:63–69.
- Chung, A.E., L.E. Estes, H. Shinozuka, J. Braginski, C. Lorz, and C.A. Chung. 1977. Morphological and biochemical observations on cells derived from the in vitro differentiation of the embryonal carcinoma cell line PCC4-F. *Cancer Res.* 37:2072–2081.
- Clem, R.J., M. Fechheimer, and L.K. Miller. 1991. Prevention of apoptosis by a baculovirus gene during infection of insect cells. *Science (Wash. DC)*. 254: 1388–1390.
- Coulombe, P.A., Y.-M. Chang, K. Albers, and E. Fuchs. 1990. Deletions in epidermal keratins leading to alterations in filament organization in vivo and in intermediate filament assembly in vitro. *J. Cell Biol.* 111:3049–3064.
- Cryns, V.L., L. Bergeron, H. Zhu, H. Li, and J. Yuan. 1996. Specific cleavage of α -Fodrin during Fas- and tumor necrosis factor-induced apoptosis is mediated by an interleukin-1 β -converting enzyme/Ced-3 protease distinct from the poly(ADP-ribose) polymerase protease. *J. Biol. Chem.* 271:31277–31282.
- Edelhoch, H. 1967. Spectroscopic determination of tryptophan and tyrosine in proteins. *Biochemistry*. 6:1948–1954.
- Einarsson, R. 1995. TPS—a cytokeratin marker for therapy control in breast cancer. *Scan. J. Clin. Lab. Invest.* 221 (Suppl.):113–115.
- Ellis, R.E., J. Yuan, and H.R. Horwitz. 1991. Mechanisms and functions of cell death. *Annu. Rev. Cell Biol.* 7:663–698.
- Emoto, Y., Y. Manome, G. Meinhardt, H. Kisaki, S. Kharbanda, M. Robertson, T. Ghayur, W.W. Wong, R. Kamen, R. Weichselbaum, and D. Kufe. 1995. Proteolytic activation of protein kinase C δ by an ICE-like protease in apoptotic cells. *EMBO (Eur. Mol. Biol. Organ.) J.* 14:6148–6156.
- Franke, W.W., E. Schmid, and C. Grund. 1982. Intermediate filament proteins in nonfilamentous structures: transient disintegration and inclusion of subunit proteins in granular aggregates. *Cell*. 30:103–113.
- Frisch, S.M., and H. Francis. 1994. Disruption of epithelial cell–matrix interactions induces apoptosis. *J. Cell Biol.* 124:619–626.
- Fuchs, E. 1997. Of mice and men: genetic disorders of the cytoskeleton. *Mol. Biol. Cell*. 8:189–203.
- Fuchs, E., and K. Weber. 1994. Intermediate filaments: structure, dynamics, function, and disease. *Annu. Rev. Biochem.* 63:345–382.
- Gagliardini, V., P.A. Fernandez, R.K.K. Lee, H. C.A. Drexler, R.J. Rotello, M.C. Fishman, and J. Yuan. 1994. Prevention of vertebrate neuronal death by crmA gene. *Science (Wash. DC)*. 263:826–828.
- Gu, Y., K. Kuida, H. Tsutsui, G. Ku, K. Hsiao, M.A. Fleming, N. Hayashi, K. Higashino, H. Okamura, K. Nakanishi, et al. 1997. Activation of interferon- γ inducing factor mediated by interleukin-1 β converting enzyme. *Science*

- (Wash. DC). 275:206–209.
- Hatzfeld, M., and W.W. Franke. 1985. Pair formation and promiscuity of cyto-keratins: formation in vitro of heterotypic complexes and intermediate-sized filaments by homologous and heterologous recombinations of purified polypeptides. *J. Cell Biol.* 101:1826–1841.
- Hembrough, T.A., J. Vasudevan, M.M. Allietta, W.F. Glass II, and S.L. Gonias. 1995. A cytokeratin 8-like protein with plasminogen-binding activity is present on the external surfaces of hepatocytes, HepG2 cells and breast carcinoma cell lines. *J. Cell Sci.* 108:1071–1082.
- Howard, A.D., M.J. Kostura, N. Thornberry, G.J.F. Ding, G. Limjoco, J. Weidner, J.P. Salley, K.A. Hogquist, D.D. Chaplin, R.A. Mumford, et al. 1991. IL-1-converting enzyme requires aspartic acid residues for processing of the IL-1 β precursor at two distinct sites and does not cleave 31-kDa IL-1 α . *J. Immunol.* 147:2964–2969.
- Inagaki, M., N. Inagaki, T. Takahashi, and Y. Takai. 1997. Phosphorylation-de-pendent control of structures of intermediate filaments: a novel approach using site- and phosphorylation state-specific antibodies. *J. Biochem.* 121: 407–414.
- Ishiwata, I., S. Nozawa, T. Inoue, and H. Okumura. 1977. Development and characterization of established cell lines from primary and metastatic regions of human endometrial carcinomas. *Cancer Res.* 37:1777–1785.
- Janicke, R.U., P.A. Walker, X.Y. Lin, and A.G. Porter. 1996. Specific cleavage of the retinoblastoma protein by an ICE-like protease in apoptosis. *EMBO (Eur. Mol. Biol. Organ.) J.* 15:6969–6978.
- Kayalar, C., T. Ord, M.P. Testa, L.-T. Zhong, and D.E. Bredesen. 1996. Cleavage of actin by interleukin 1 β -converting enzyme to reverse DNase I inhibition. *Proc. Natl. Acad. Sci. USA.* 93:2234–2238.
- Klymkowsky, M.W., L.A. Maynell, and C. Nislow. 1991. Cytokeratin phosphorylation, cytokeratin filament severing and the solubilization of the maternal mRNA Vg1. *J. Cell Biol.* 114:787–797.
- Ku, N.-O., and M.B. Omary. 1994. Identification of the major physiologic phosphorylation site of human keratin 18: potential kinases and a role in filament reorganization. *J. Cell Biol.* 127:161–171.
- Ku, N.-O., S. Michie, R.G. Oshima, and M.B. Omary. 1995. Chronic hepatitis, hepatocyte fragility, and increased soluble phosphoglycokeratins in transgenic mice expressing a keratin 18 conserved arginine mutant. *J. Cell Biol.* 131:1303–1314.
- Ku, N.-O., J. Liao, C.-F. Chou, and M.B. Omary. 1996a. Implications of intermediate filament protein phosphorylation. *Cancer Metastasis Rev.* 15:429–444.
- Ku, N.-O., S. Michie, R. Soetikno, E. Resurreccion, R.G. Oshima, and M.B. Omary. 1996b. Susceptibility to hepatotoxicity in transgenic mice that express a dominant-negative human keratin 18 mutant. *J. Clin. Invest.* 98:1034–1046.
- Kulesh, D.A., and R.G. Oshima. 1988. Cloning of the human keratin 18 gene and its expression in non-epithelial mouse cells. *Mol. Cell. Biol.* 8:267–272.
- Kulesh, D.A., G. Cecena, Y.M. Darmon, M. Vasseur, and R.G. Oshima. 1989. Post-translational regulation of keratins: degradation of unpolymerized mouse and human keratins 18 and 8. *Mol. Cell. Biol.* 9:1553–1565.
- Kumar, S., and M.F. Lavin. 1996. The ICE family of cysteine proteases as effectors of cell death. *Cell Death Diff.* 3:255–267.
- Laemmli, U.K. 1970. Cleavage of structural proteins during the assembly of the head of bacteriophage T4. *Nature (Lond.)*. 227:680–685.
- Lazebnik, Y.A., S.H. Kaufmann, S. Desnoyers, G.G. Poirier, and W.C. Earnshaw. 1994. Cleavage of poly(ADP-ribose) polymerase by a proteinase with properties like ICE. *Nature (Lond.)*. 371:346–347.
- Liao, J., and M.B. Omary. 1996. 14-3-3 proteins associate with phosphorylated simple epithelial keratins during cell cycle progression and act as a solubility cofactor. *J. Cell Biol.* 133:345–357.
- Liao, J., L.A. Lowthert, N.-O. Ku, R. Fernandez, and M.B. Omary. 1995a. Dynamics of human keratin 18 phosphorylation: polarized distribution of phosphorylated keratins in simple epithelial tissues. *J. Cell Biol.* 131:1291–1301.
- Liao, J., L.A. Lowthert, and M.B. Omary. 1995b. Heat stress or rotavirus infection of human epithelial cells generates a distinct hyperphosphorylated form of keratin 8. *Exp. Cell Res.* 219:348–357.
- Machiels, B.M., M.E.R. Henfling, B. Schutte, M. Van Engeland, J.L.V. Broers, and F.C.S. Ramaekers. 1996. Subcellular localization of proteasomes in apoptotic lung tumor cells and persistence as compared to intermediate filaments. *Eur. J. Cell Biol.* 70:250–259.
- Martin, S.J., and D.R. Green. 1995. Protease activation during apoptosis: death by a thousand cuts? *Cell.* 82:349–352.
- Martin, S.J., C.P.M. Reutelingsperger, A.J. McGahon, J.A. Rader, R.C.A.A. van Schie, D.M. LaFace, and D.R. Green. 1995. Early redistribution of a plasma membrane phosphatidylserine is a general feature of apoptosis regardless of the initiating stimulus: inhibition by overexpression of Bcl-2 and Abl. *J. Exp. Med.* 182:1545–1556.
- Miossec, C., V. Dutileul, F. Fassy, and A. Diu-Hercend. 1997. Evidence for CPP32 activation in the absence of apoptosis during T lymphocyte stimulation. *J. Biol. Chem.* 272:13459–13462.
- Miura, M., H. Zhu, R. Rotello, E.A. Hartwig, and J. Yuan. 1993. Induction of apoptosis in fibroblasts by 1L-1 β -converting enzyme, a mammalian homolog of the *C. elegans* cell death gene ced-3. *Cell.* 75:653–660.
- Na, S., T.-H. Chuang, A. Cunningham, T.G. Turi, J.H. Hanke, G.M. Bokoch, and D.E. Danley. 1996. D4-GDI, a substrate of CPP32, is proteolyzed during Fas-induced apoptosis. *J. Biol. Chem.* 271:11209–11213.
- Orth, K., K. O'Rourke, G.S. Salvesen, and V.M. Dixit. 1996. Molecular ordering of apoptotic mammalian CED-3/ICE-like proteases. *J. Biol. Chem.* 271: 20977–20980.
- Oshima, R.G. 1981. Identification and immunoprecipitation of cytoskeletal proteins from murine extra-embryonic endodermal cells. *J. Biol. Chem.* 256: 8124–8133.
- Oshima, R.G. 1982. Developmental expression of murine extra-embryonic endodermal cytoskeletal proteins. *J. Biol. Chem.* 257:3414–3421.
- Oshima, R.G., J.L. Millan, and G. Cecena. 1986. Comparison of mouse and human keratin 18: a component of intermediate filaments expressed prior to implantation. *Differentiation.* 33:61–68.
- Oshima, R.G., L. Abrams, and D. Kulesh. 1990. Activation of an intron enhancer within the keratin 18 gene by expression of c-fos and c-jun in undifferentiated F9 embryonal carcinoma cells. *Genes Dev.* 4:835–848.
- Oshima, R.G., H. Baribault, and C. Caulin. 1996. Oncogenic regulation and function of keratin 8 and 18. *Cancer Metastasis Rev.* 15:445–471.
- Pankov, R., I. Simcha, M. Zoller, R.G. Oshima, and A. Ben-Ze'ev. 1997. Contrasting effects of K8 and K18 on stabilizing K19 expression, cell motility and tumorigenicity in the BSp73 adenocarcinoma. *J. Cell Sci.* 110:965–974.
- Parekh, H.K., and H. Simpkins. 1995. The differential expression of cytokeratin 18 in cisplatin-sensitive and -resistant human ovarian adenocarcinoma cells and its association with drug sensitivity. *Cancer Res.* 55:5203–5206.
- Rabizadeh, S., D.J. LaCount, P.D. Friesen, and D.E. Bredesen. 1993. Expression of the baculovirus p35 gene inhibits mammalian neural cell death. *J. Neurochem.* 61:2318–2321.
- Rao, L., D. Perez, and E. White. 1996. Lamin proteolysis facilitates nuclear events during apoptosis. *J. Cell Biol.* 135:1441–1455.
- Ray, C.A., R.A. Black, S.R. Kronheim, T.A. Greenstreet, P.R. Sleath, G.S. Salvesen, and D.J. Pickup. 1992. Viral inhibition of inflammation: cowpox virus encodes an inhibitor of the interleukin-1 β converting enzyme. *Cell.* 69: 597–604.
- Rees, S., J. Coote, J. Stables, S. Goodson, S. Harris, and M.G. Lee. 1996. Bicistronic vector for the creation of stable mammalian cell lines that predisposes all antibiotic-resistant cells to express recombinant protein. *BioTechniques.* 20:102–110.
- Rugg, E.L., S.M. Morley, F.J.D. Smith, M. Boxer, M.J. Tidman, H. Navsaria, I.M. Leigh, and E.B. Lane. 1993. Missing links: Weber-Cockayne keratin mutations implicate the L12 linker domain in effective cytoskeleton function. *Nat. Genet.* 5:294–300.
- Rydlander, L., E. Ziegler, T. Bergman, E. Schöberl, G. Steiner, A.C. Bergman, A. Zetterberg, M. Marberger, P. Björklund, T. Skern, et al. 1996. Molecular characterization of a tissue-polypeptide-specific-antigen epitope and its relationship to human cytokeratin 18. *Eur. J. Biochem.* 241:309–314.
- Schaafsma, H.E., F.C. Ramaekers, G.N. van Muijen, E.B. Lane, I.M. Leigh, H. Robben, A. Huijssmans, and E.C. Ooms. 1990. Distribution of cytokeratin polypeptides in human transitional cell carcinomas, with special emphasis on changing expression patterns during tumor progression. *Am. J. Pathol.* 136: 329–343.
- Schussler, M.H., A. Skoudy, F. Ramaekers, and F.X. Real. 1992. Intermediate filaments as differentiation markers of normal pancreas and pancreas cancer. *Am. J. Pathol.* 140:559–568.
- Singer, P.A., K. Trevor, and R.G. Oshima. 1986. Molecular cloning and characterization of the Endo B cytokeratin expressed in preimplantation mouse embryos. *J. Biol. Chem.* 261:538–547.
- Song, Q., S.P. Lees-Miller, S. Kumar, N. Zhang, D.W. Chan, G.C.M. Smith, S.P. Jackson, E.S. Alnemri, G. Litwack, K.K. Khanna, and M.F. Lavin. 1996. DNA-dependent protein kinase catalytic subunit: a target for an ICE-like protease in apoptosis. *EMBO (Eur. Mol. Biol. Organ.) J.* 15:3238–3246.
- Steinert, P.M., and D.R. Roop. 1988. Molecular and cellular biology of intermediate filaments. *Annu. Rev. Biochem.* 57:593–625.
- Steinert, P.M., W.W. Idler, and S.B. Zimmerman. 1976. Self-assembly of bovine keratin filaments in vitro. *J. Mol. Biol.* 108:547–567.
- Sugimoto, A., P.D. Friesen, and J.H. Rothman. 1994. Baculovirus p35 prevents developmentally programmed cell death and rescues a ced-9 mutant in the nematode *Caenorhabditis elegans*. *EMBO (Eur. Mol. Biol. Organ.) J.* 13: 2023–2028.
- Takahashi, A., E.S. Alnemri, Y.A. Lazebnik, T. Fernandes-Alnemri, G. Litwack, and R.D. Moir. 1996. Cleavage of lamin A by Mch2 α but not CPP32: multiple interleukin 1 β -converting enzyme-related proteases with distinct substrate recognition properties are active in apoptosis. *Proc. Natl. Acad. Sci. USA.* 93:8395–8400.
- Thiagarajan, P., and J.F. Tait. 1990. Binding of annexin V/placental anticoagulant protein I to platelets. *J. Biol. Chem.* 265:17420–17423.
- Thompson, C.B. 1995. Apoptosis in the pathogenesis and treatment of disease. *Science (Wash. DC)*. 267:1456–1462.
- Toivola, D.M., R.D. Goldman, D.R. Garrod, and J.E. Eriksson. 1997. Protein phosphatases maintain the organization and structural interactions of hepatic keratin intermediate filaments. *J. Cell Sci.* 110:23–33.
- Towbin, H., T. Staehelin, and J. Gordon. 1979. Electrophoretic transfer of proteins from polyacrylamide gels to nitrocellulose sheets: procedure and some applications. *Proc. Natl. Acad. Sci. USA.* 76:4350–4354.
- Trask, D.K., V. Band, D.A. Zajchowski, P. Yaswen, T. Suh, and R. Sager. 1990. Keratins as markers that distinguish normal and tumor-derived mammary epithelial cells. *Proc. Natl. Acad. Sci. USA.* 87:2319–2323.
- Trevor, K., and R.G. Oshima. 1985. Preimplantation mouse embryos and liver

- express the same type I keratin gene product. *J. Biol. Chem.* 260:15885–15891.
- Wang, X., N.G. Zelenski, G. Yang, J. Sakai, M.S. Brown, and J.L. Goldstein. 1996. Cleavage of sterol regulatory element binding proteins (SREBPs) by CPP32 during apoptosis. *EMBO (Eur. Mol. Biol. Organ.) J.* 15:1012–1020.
- Weber, K., M. Osborn, R. Moll, B. Wickland, and B. Luning. 1984. Tissue polypeptide antigen (TPA) is related to the non-epidermal keratins 8.18 and 19 typical of simple and non-squamous epithelia: re-evaluation of a human tumor marker. *EMBO (Eur. Mol. Biol. Organ.) J.* 3:2707–2714.
- Wyllie, A.H., J.F.R. Kerr, and A.R. Currie. 1980. Cell death: the significance of apoptosis. *Int. Rev. Cytol.* 68:251–306.
- Xue, D., and H.R. Horvitz. 1995. Inhibition of the *Caenorhabditis elegans* cell-death protease CED-3 by a CED-3 cleavage site in baculovirus p35 protein. *Nature (Lond.)*. 377:248–251.
- Yuan, J., S. Shaham, S. Ledoux, H.M. Ellis, and H.R. Horvitz. 1993. The *C. elegans* cell death gene *ced-3* encodes a protein similar to mammalian interleukin-1 β -converting enzyme. *Cell.* 75:641–652.